Development of Asymmetric Photochemical Reaction of Electron-Rich Cyclopropanols and Electron-Deficient Alkenes

Bachelor thesis

Student: Rasmus Käsper
Student code: 213023LAAB
Supervisors: Anastasiya Krech, PhD student, Department of Chemistry and Biotechnology;
Maksim Ošeka, Assistant Professor, Department of Chemistry and Biotechnology
Study program: LAAB17/20 – Applied Chemistry and Gene Technology

Tallinn 2024

Elektron-rikaste tsüklopropanoolide ja elektron-vaeste alkeenide asümmeetrilise fotokeemilise reaktsiooni arendamine

Bakalaureusetöö

Üliõpilane: Rasmus Käsper
Üliõpilaskood: 213023LAAB
Juhendajad: Anastasiya Krech, doktorant-nooremteadur, Keemia ja Biotehnoloogia instituut;
Maksim Ošeka, nooremprofessor, Keemia ja Biotehnoloogia instituut
Õppekava: LAAB17/20 – Rakenduskeemia ja geenitehnoloogia

Tallinn 2024

Declaration

Hereby I declare that I have compiled the paper independently and all works, important standpoints and data by other authors have been properly referenced and the same paper has not been previously presented for grading.

Author: Rasmus Käsper

[Signature, date]
Signed digitally

The paper conforms to requirements in force.

Supervisor: Anastasiya Krech

[Signature, date]
Signed digitally

Table of Contents

List of Abbreviations

Boc – *tert*-butyloxycarbonyl

DAST – diethylaminosulfur trifluoride

DIAD – diisopropyl azodicarboxylate

DMAP – 4-(dimethylamino)pyridine

DPPA – diphenylphosphoryl azide

EDA – electron donor-acceptor

FEP – fluorinated ethylene-propylene

HAT – hydrogen atom transfer

HPLC – high-performance liquid chromatography

IUPAC – International Union of Pure and Applied Chemistry

LED – light-emitting diode

NFSI – *n*-fluorobenzenesulfomide

NMR – nuclear magnetic resonance

OTf – trifluoromethanesulfonate

ppm – parts per million

PyBox – pyridine bis(oxazoline)

SET – single-electron transfer

TBADT – tetrabutylammonium decatungstate

TLC – thin-layer chromatography

UV – ultraviolet

1. Introduction

Green chemistry, also referred to as sustainable chemistry, is the way for chemists to prevent polluting and harming our planet. The twelve principles of green chemistry, developed by Paul Anastas and John Warner in 1998, provide a framework for learning about and applying green chemistry.[1] The principles outline ways to reduce waste, design efficient reactions and perform safer chemistry. In this work, we aim to implement these principles to develop a reaction, using light as an efficient green energy source and organocatalysts instead of transition metal catalysts that may be toxic.

Organic photochemistry is the tool used by synthetic chemists to develop green reactions. The absorption of light excites molecules of substrates, photosensitisers or photocatalysts, which often leads reactions to occur without additional thermal activation. This makes the usage of photochemistry a great advantage, since working at low temperatures usually increases the selectivity, thus avoiding side reactions.

The chirality of a molecule is of utmost importance in the biochemistry of living organisms as well as in the field of pharmaceuticals. There are many examples of chiral drugs, where one enantiomer has the desired effect, but the other one is toxic or results in undesirable side effects. Hence, developing highly enantioselective reactions is necessary for the development of new chiral drugs, which may help combat illnesses in ways not possible before. Our objective was to combine enantioselective synthesis with green chemistry. Developing an enantioselective reaction which is not wasteful, can easily be scaled up and does not necessitate the use of expensive catalysts and reagents is a goal for current and future organic chemists.

In this work we aimed to develop an asymmetric photochemical reaction of an electron-rich cyclopropanol and an electron-deficient alkene without the addition of external photocatalyst (Scheme 1). The Ošeka group has recently shown the formation of an electron donor-acceptor (EDA) complex between the cyclopropanol and the alkene, and their consequent reaction under the 370 nm ultraviolet (UV) light.[2] Due to the reacting alkenes being Michael acceptors, we envisioned the possibility of inducing enantioselectivity in this reaction with the addition of chiral bifunctional organocatalysts.

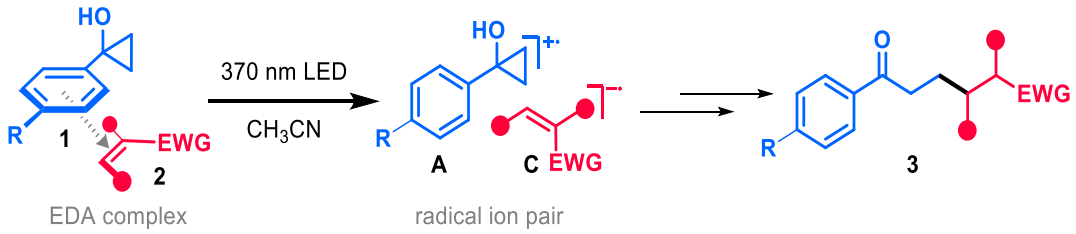

Scheme 1. The outline of this work.

2. Literature review

2.1 Photochemistry and photoredox catalysis

According to the International Union of Pure and Applied Chemistry (IUPAC), a photochemical reaction is a chemical reaction caused by absorption of ultraviolet, visible or infrared irradiation.[3] The first reaction triggered solely by the absorption of light energy and not involving a thermal activation, was carried out by Joseph Priestley in the eighteenth century (Scheme 2).[4] It was a reaction in the field of inorganic chemistry, involving the light irradiation of nitric acid vapors, which converted into nitrogen dioxide and dissolved into the liquid nitric acid, giving it a reddish color.

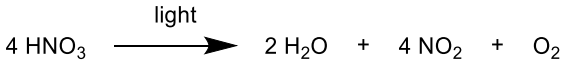

Scheme 2. Light decomposition of nitric acid.

Giacomo Ciamician is widely regarded as one of the pioneers of organic photochemistry. In the beginning of 20th century, he stated that the world would need to move to renewable energy to make itself independent from coal, which he claimed would be completely exhausted in the future. Ciamician envisioned the possibility to use photochemical devices utilizing solar energy to power the human civilization and urged humanity to develop such devices. His work on photochemistry included discoveries of cycloaddition (Scheme 3 a) and geometric isomerization reactions (Scheme 3 b).[5]

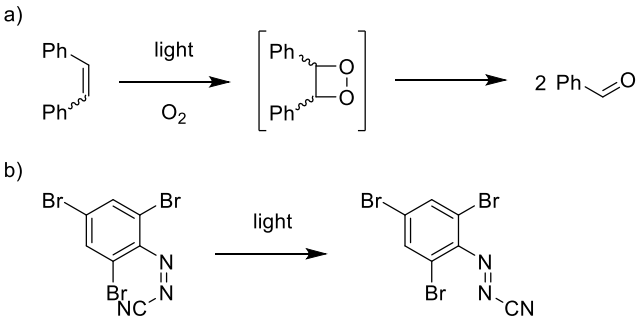

Scheme 3. Examples of Giacomo Ciamician's photochemical reactions. a) Photochemical cycloaddition reaction, b) Light-induced geometric isomerization of a double bond.

Light is used in organic chemistry as a method of bringing molecules into an electronically excited state. In such a state, the chemical properties of the molecules change, and various chemical reactions may occur. Photochemical activation offer the formation of thermodynamically disfavoured products compared to the thermal activation, therefore allowing reactivity otherwise inaccessible by thermal methods.[3] In many cases, the photochemical transformation of organic molecules involves the formation of radical species.

A radical is a molecule possessing an unpaired electron (Scheme 4 a).[6] A pair of radicals are formed through breakage of weak bonds or electron transfer. After formation, radicals can undergo one of three types of reactions – abstraction, addition, and elimination (Scheme 4 b).

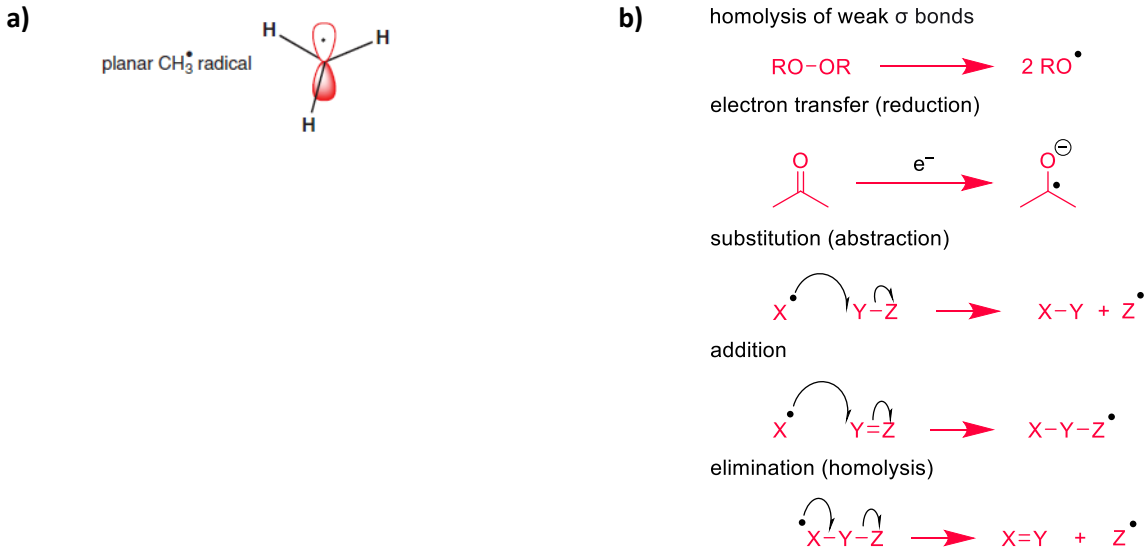

Scheme 4. a) The structure of a radical. b) Examples of the formation of the radicals and their reactions.

The development of precise light-emitting diodes (LEDs) has revolutionized the field of photochemistry by providing researchers with an accurate (narrow-emission), energy-efficient, and easily adjustable light source for a broad range of applications, driving increased interest and advancements in this field. Photochemical reactions can be carried out under UV or visible-light irradiation. UV light can directly activate the molecules (such as aromatic molecules) and trigger intramolecular or intermolecular transformations, for example 4π- and 6π-photocyclization, hydrogen-atom abstraction, and 2+2 photocycloaddition reactions.[7]

While generally not absorbed by most organic molecules, visible light can be utilized in light-mediated reactions through the use of photocatalysts. Transition metal complexes or organic photocatalysts (Figure 1) absorb light to transform into an excited state to then catalyse the reaction between substrates. The use of transition metal complexes as catalysts for photochemical reactions in organic chemistry has gained traction in the late 2000s, thanks to the efforts of the Yoon, Stephenson and MacMillan groups.[8]

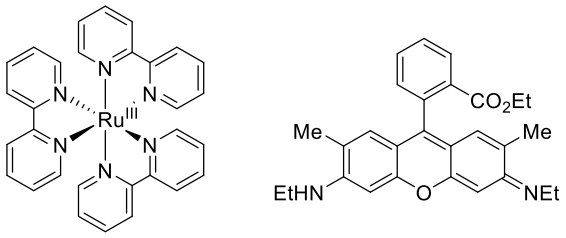

Figure 1. Examples of transition metal complexes and organic photocatalysts.

2.2 Reactivity of electron donor-acceptor (EDA) complexes

One important strategy in organic photochemistry is the use of EDA complex reactivity under irradiation (Scheme 5).[9] An electron donor-acceptor complex can be formed from an electron-rich and an electron-poor molecule. Under irradiation by UV or visible light, an electron transfer can occur within the EDA complex without the need for a photocatalyst to be present. A generated radical ion pair (radical anion and radical cation) can undergo different reaction pathways such as additions, eliminations and rearrangements or generate free radical ions.[10]

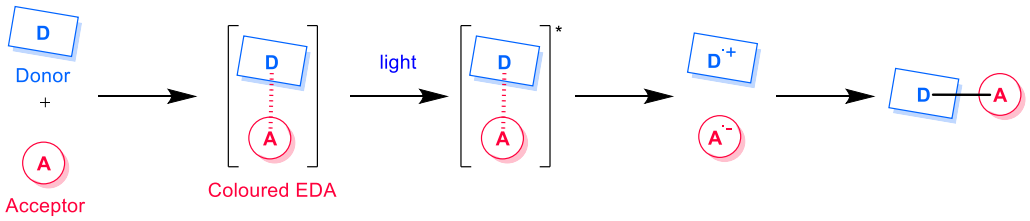

Scheme 5. EDA complex reactivity under irradiation.

In 2013, the Melchiorre group showed that chiral EDA complexes can be an integral part of asymmetric transformations, in their case the α-alkylation of aldehydes with alkyl halides (Scheme 6).[11] The reported reaction could not be realized through a thermal pathway and necessitated visible light to complete the reaction. Hence, highly organized EDA complexes can be a connection between asymmetric synthesis and photochemistry.

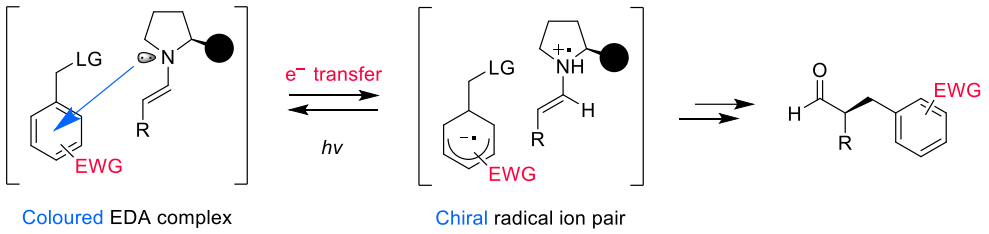

Scheme 6. α-Alkylation of aldehyde with alkyl halide via EDA complex.

In 2023, the Ošeka group reported a tetrabutylammonium decatungstate (TBADT) photocatalyzed reaction between cyclopropanols and electron-deficient alkenes (Scheme 7).[2] The decatungstate anion $[W_{10}O_{32}]^{4-}$ is a widely used photocatalyst for promoting hydrogen atom transfer (HAT) reactions under UV light irradiation.[12–15] However, the Ošeka group found that TBADT is also able to directly oxidize cyclopropanols via the single-electron transfer (SET) mechanism. The group also disclosed the formation of EDA complexes between electron-rich aromatic cyclopropanols and electron-deficient alkenes, which allow the reaction to proceed under UV light irradiation via the photoinduced charge transfer without the usage of a photocatalyst to facilitate the reaction (Scheme 7).[2]

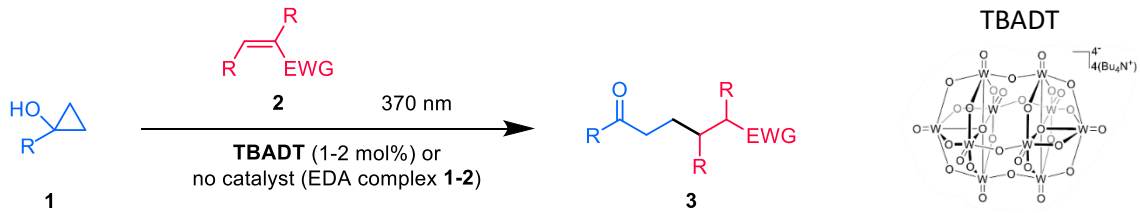

Scheme 7. The photochemical reaction between cyclopropanol and electron-deficient alkene and the structure of the TBADT photocatalyst.

2.3 Asymmetric organocatalysis

In organic synthesis, transition metal catalysts are often used for performing various transformations. However, the transition metals catalysts can be toxic, expensive and they are often unstable to atmospheric conditions or sensitive to moisture. For synthetic organic chemistry, the use of small organic molecules known as organocatalysts can be the solution. Organocatalysts are generally not as toxic compared to transition metal catalysts. For enantioselective synthesis, chiral organocatalysts may be used, many of which are either easily available from biological sources as single enantiomers or are cheap to prepare compared to the transition metals.[16]

Asymmetric organocatalysis can use several modes of activation: covalent-bonding (i.e. enamine catalysis and iminium catalysis) and non-covalent bonding catalysis (such as hydrogen-bonding and phase transfer catalysis). Hydrogen bonding (Figure 2) is an attractive interaction between a hydrogen atom that is covalently bonded to a more electronegative atom, and another electronegative atom with an electron pair which can accept the hydrogen bond. Nitrogen, oxygen and fluorine are the most prevalent hydrogen bond acceptors in organic molecules. Hydrogen bonding can be both intermolecular and intramolecular.

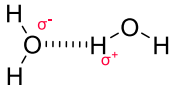

Figure 2. Example of a hydrogen bond between two H_2O molecules.

Hydrogen-bond catalysis is a type of organocatalysis relying on hydrogen bonding interactions to control and accelerate organic reactions. Bifunctional organocatalysts are an example, forming multiple hydrogen bonds with the substrate in a reaction (Scheme 8). The functional groups in the organocatalysts can both donate or accept hydrogen bonds, which stabilize the substrates in a specific way to induce enantioselectivity.

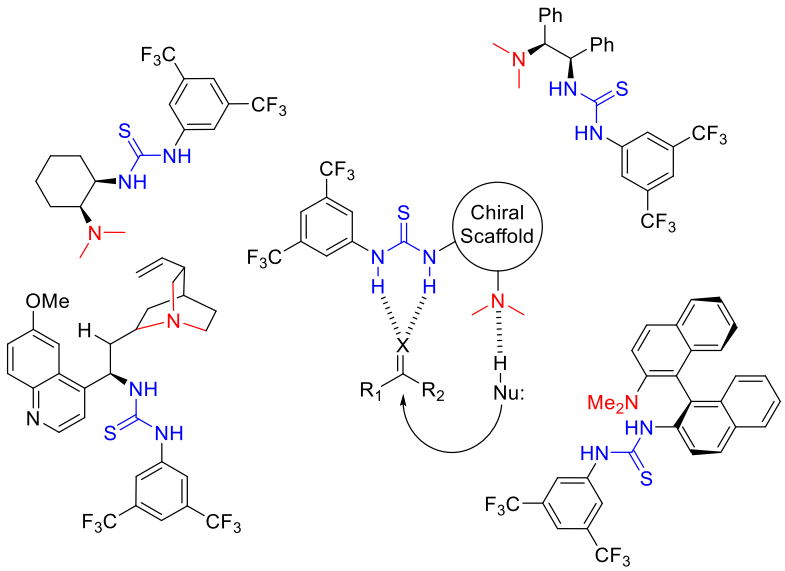

Scheme 8. Examples of hydrogen bonding amine-thiourea catalysts and the substrate activation model.

3. Results and discussion

Our research aimed to develop an asymmetric photochemical reaction of an electron-rich cyclopropanol and an electron-deficient alkene. The Ošeka group showed the reaction before with the formation of an EDA complex between the cyclopropanol and the alkene under 370 nm UV light irradiation.[2] As the reacting alkenes are also well-known Michael acceptors, we envisioned the possibility of developing an asymmetric version of this reaction with the addition of bifunctional hydrogen-bonding chiral organocatalysts.

3.1 Synthesis of starting materials

3.1.1 Cyclopropanol synthesis

The synthesis of cyclopropanol **5** was carried out by the Kulinkovich reaction.[18] First, the Grignard reagent ethylmagnesium bromide was synthesized from ethyl bromide and magnesium turnings with 96% yield. Then, methyl 4-methoxybenzoate **4** reacted with methylmagnesium bromide, ethylmagnesium bromide and titanium isopropoxide ($Ti(OiPr)_4$) to form cyclopropanol **5** with 49% yield (Scheme 9).

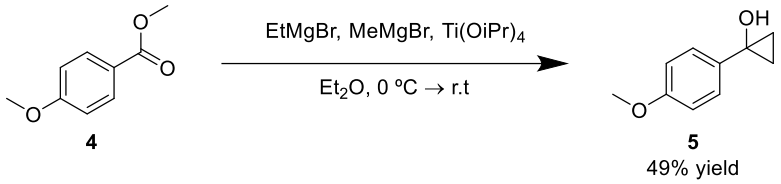

Scheme 9. Synthesis of 1-(4-methoxyphenyl)cyclopropan-1-ol.

3.1.2 Synthesis of Michael acceptors

Commercially available benzaldehyde **6** and malononitrile **7** were treated with sodium methoxide (NaOMe) to obtain benzylidene malononitrile **8** with 85% yield (Scheme 10).

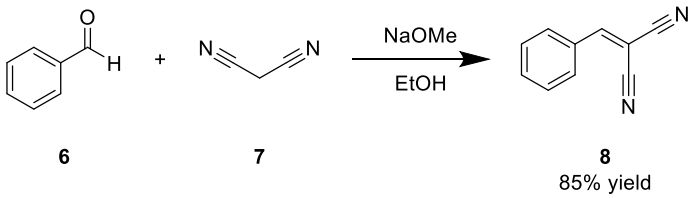

Scheme 10. Synthesis of benzylidene malononitrile.

(*E*)-3-benzylideneindolin-2-one **10** was synthesized from commercially available benzaldehyde **6** and indolin-2-one **9** using pyrrolidine as a catalyst with 63% yield (Scheme 11).

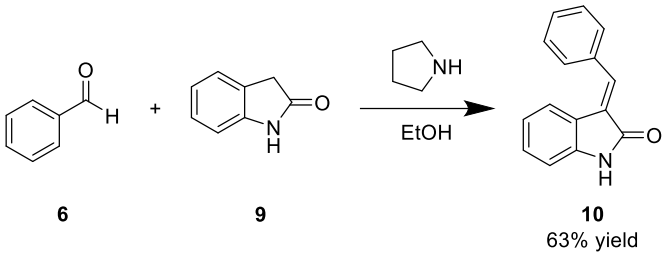

6 **9** **10**
63% yield

Scheme 11. Synthesis of (Z)-3-benzylideneindolin-2-one.

Oxindole **13** was synthesized from commercially available isatin **11**. First, the amino group was protected with *tert*-butyloxycarbonyl (Boc) group to obtain Boc-protected isatin **12** with 31% yield, which then underwent the Wittig reaction with phosphonium ylide to obtain **13** with 70% yield (Scheme 12).

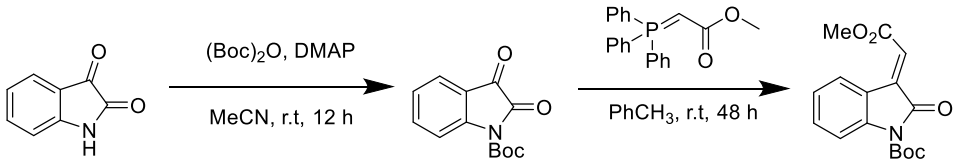

11 **12**
31% yield
13
70% yield

Scheme 12. Synthesis of *tert*-butyl (*E*)-3-(2-methoxy-2-oxoethylidene)-2-oxoindoline-1-carboxylate **13**.

Another potential alkene for a photochemical reaction, difluorovinylbenzonitrile **15,** was synthesized from 4-formylbenzonitrile **14**, sodium chlorodifluoroacetate and triphenyl phosphine (PPh_3) with 40% yield (Scheme 13).

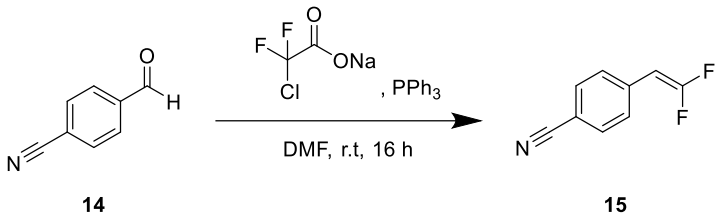

14 **15**
40% yield

Scheme 13. Synthesis of 4-(2,2-difluorovinyl)benzonitrile **15**.

3.1.3 Synthesis of catalysts

9-amino(9-deoxy)epihydroquinine **18** was synthesized according to the literature procedure.[19] Quinine **16** was first hydrogenated under continuous flow conditions using H-Cube® (Figure 3) to obtain dihydroquinine **17** with 75% yield (Scheme 14). H-Cube® is a flow reactor that generates hydrogen gas on demand through water electrolysis using sealed palladium-carbon catalyst cartridges, enabling fast reactions with a high level of safety.

Figure 3. ThalesNano H-Cube® flow reactor.

Then, Mitsunobu and then Staudinger reactions were consequently performed in one-pot on dihydroquinine **17** to transform the alcohol group into amine and inverse its configuration, thus obtaining 9-amino(9-deoxy)epihydroquinine **18.** Compound **18** was transformed into its ammonium chloride salt and recrystallized for purification and subsequently neutralized to obtain compound **18** back with 80% yield (Scheme 14).

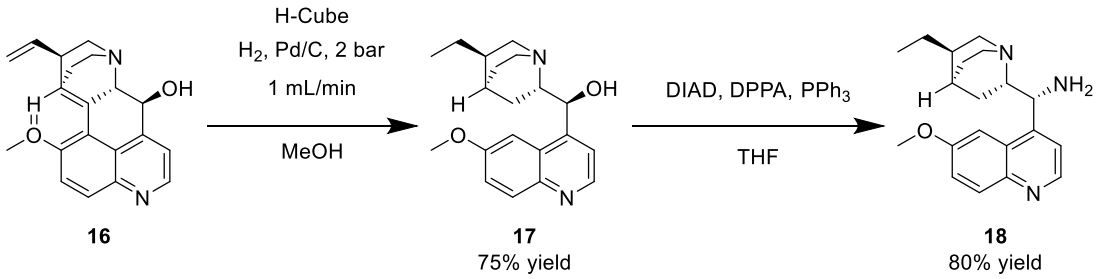

Scheme 14. Synthesis of 9-amino(9-deoxy)epihydroquinine **18**.

To obtain squaramide-based organocatalyst **20** with 81% yield, amine **18** reacted with squaramide derivative **19** (Scheme 15). Product **20** was later used in photochemical reactions.

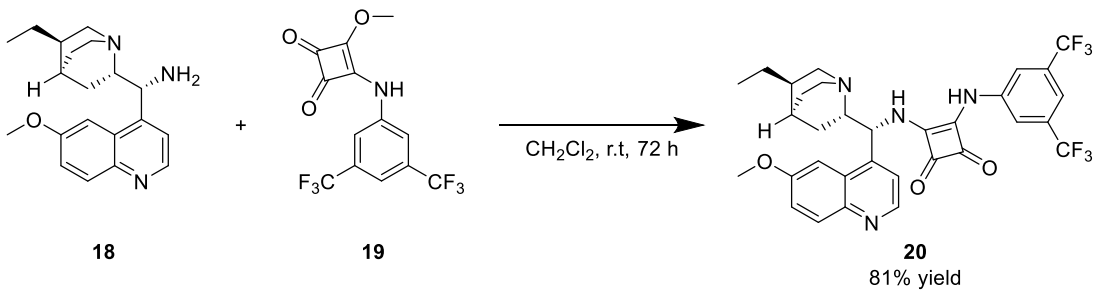

Scheme 15. Synthesis of organocatalyst **20**.

Thiourea-based organocatalyst **22** was synthesized from amine **18** and isothiocyanate **21** with 33% yield, and was also used in photochemical reactions (Scheme 16).

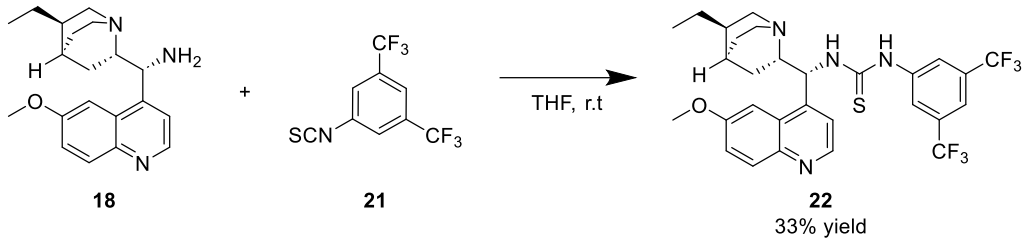

Scheme 16. Synthesis of organocatalyst **22**.

3.2 Photochemical reaction optimization in batch

All photochemical reactions were conducted in 10 mL Schlenk tubes, using photochemical reactor A (370 nm) or B (395 nm) depending on the irradiation wavelength with both reactors being air cooled and placed on top of a magnetic stirrer (Figure 4). For reaction optimization, cyclopropanol **5** was taken as a model electron-rich substrate. Five different bifunctional organocatalysts were tested in the EDA-complex-based photochemical reactions (Figure 5). Additionally, Lewis acid catalysis (scandium trifluoromethanesulfonate ($Sc(OTf)_3$) with pyridine bis(oxazoline) (PyBox) ligand) was explored to induce chirality in the product (Figure 6). The objective of this reaction optimization was to achieve as high an enantioselectivity as possible while maintaining an acceptable yield.

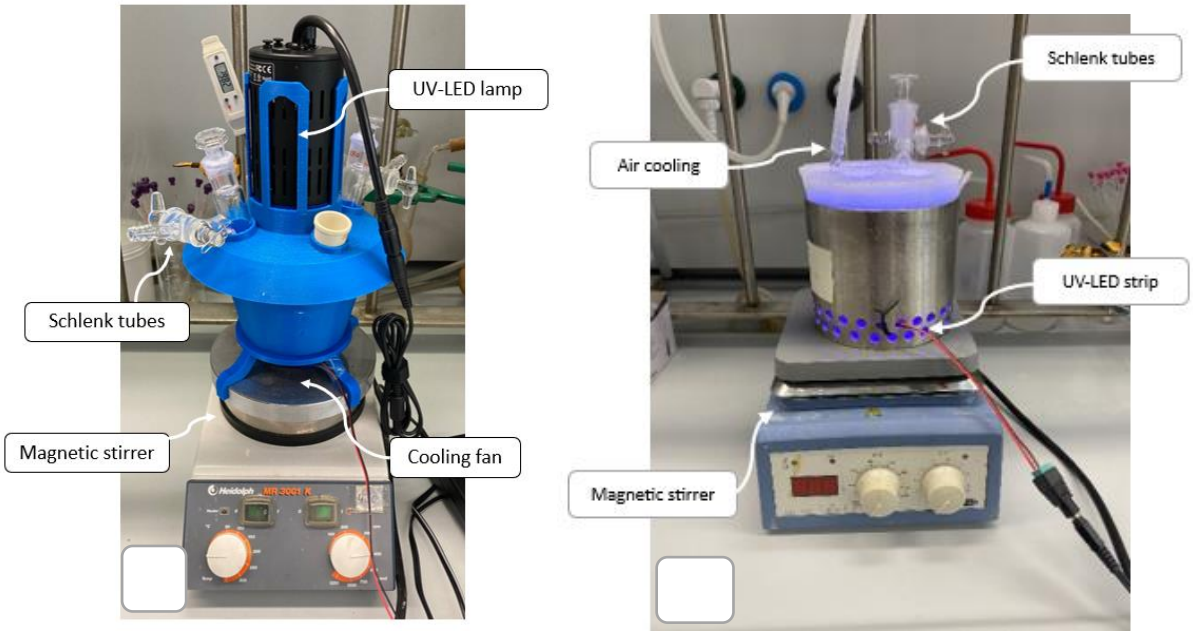

Figure 4. Photochemical reactors A and B used for reaction optimization.

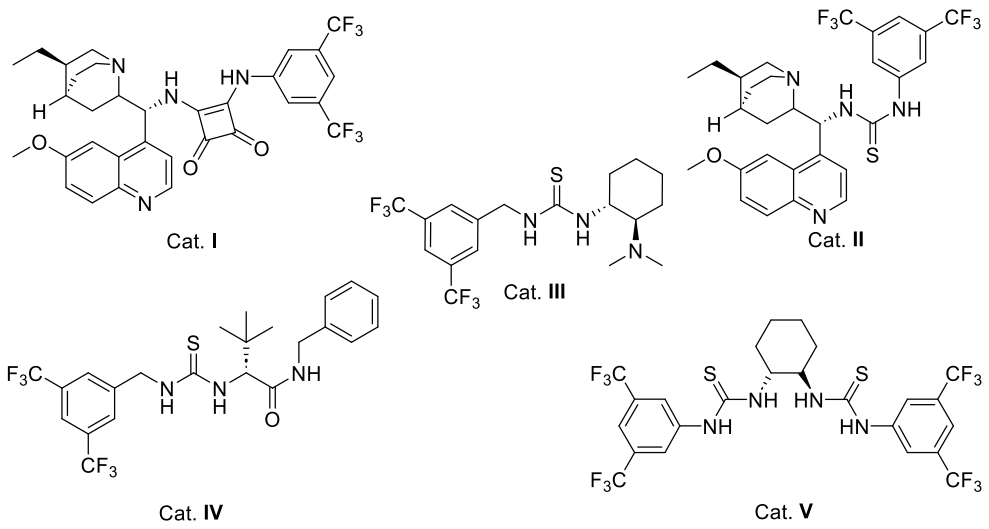

Figure 5. Bifunctional hydrogen-bonding organocatalysts used in this work.

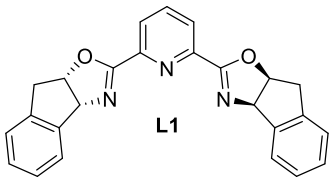

Figure 6. PyBox ligand used in this work.

First, control experiments were performed with alkenes **10** and **15**. Their photochemical reaction with cyclopropanol **5** showed no reactivity and due to those results the alkenes were not used for further optimization.

Then, benzylidene malononitrile **8** and cyclopropanol **5** were used to perform the photochemical reaction in dichloromethane under 370 nm irradiation. With all four different catalysts, this reaction gave low yields and no enantioselectivity was achieved except for the catalyst **III**, which gave a very low enantioselectivity (*ee* 7%) of the product **23** (Table 1, entries 1-4). Due to these results, alkene **5** was not used for photochemical reaction optimization any further.

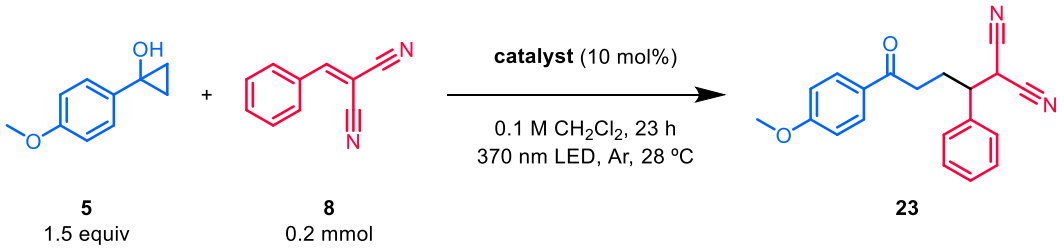

Entry	Catalyst	NMR yield, %[b]	*ee*, %[c]
1	Cat. **I**	28	racemic
2	Cat. **II**	26	racemic
3	Cat. **III**	25	7
4	Cat. **IV**	26	racemic

Table 1.[a] Reaction optimization in batch. [a] Reaction conditions: alkene **8** (0.2 mmol), cyclopropanol **5** (1.5 equiv.), catalyst (10 mol%), 0.1 M CH_2Cl_2, 370 nm LED, under Ar, 28 °C, 23 h. The reactions were performed in reactor A with 370 nm irradiation. [b] Yield was determined by ^1H NMR analysis of the crude reaction mixture against triphenylmethane as an internal standard. [c] *ee* was determined by chiral HPLC analysis.

Next, a control experiment with alkene **13** was performed at 370 nm without addition of a catalyst. Product **24** was obtained in 26% NMR yield and was racemic. (Table 2, entry 1). Then, $Sc(OTf)_3$ together with a PyBox ligand **L1** were added to see if a Lewis acid catalyst could introduce enantioselectivity in this reaction. This gave a low yield (17%) and enantioselectivity (*ee* 10%/14%) with a diastereomeric ratio of 1.4:1 (Table 2, entry 2). Afterwards, the focus was put on using hydrogen-bonding organocatalysts. Bifunctional thiourea-based catalyst **V** gave 21% yield of the ketone **24** (Table 2, entry 3) and only achieved major diastereomer enantioselectivity (*ee* 13%/0%) with a diastereomeric ratio of 1.8:1, therefore catalyst **V** was no longer used. The reaction with bifunctional squaramide-derived catalyst **I** gave product **24** with 24% yield, very low enantioselectivity (*ee* 10%/3%) and a diastereomeric ratio of 1.6:1 (Table 2, entry 4). Due to these results, the amount of catalyst **I** was increased to 20 mol%, which gave a similar yield of the ketone **24** (26%), but higher enantioselectivity compared to the previous experiments (*ee* 13%/19%) with a diastereomeric ratio of 1.2:1 (Table 2, entry 5). The addition of TBADT as a photocatalyst gave a similarly low diastereomeric ratio of 1.3:1 and moderate yield (48%) but lower enantioselectivity (*ee* 6%/10%) (Table 2, entry 6). The addition of catalyst **II** was slightly more beneficial for the enantioselectivity (*ee* 13%/22%) and a diastereomeric ratio of 1.6:1 (Table 2, entry 7). Lastly, two experiments were conducted at 395 nm in the reactor B. This wavelength was chosen as a milder light source to avoid side product formation. Catalyst **I** was used for both reactions, the difference this time being the solvent. In dichloromethane, a higher yield (39%), slightly lower enantioselectivity (13%/12%) and diastereomeric ratio of 1.6:1 was achieved (Table 2, entry 8). The usage of toluene gave a similar yield (29%), enantioselectivity (*ee* 16%/16%) and diastereomeric ratio (1.4:1) (Table 2, entry 9). All experiments showed full conversions of starting materials.

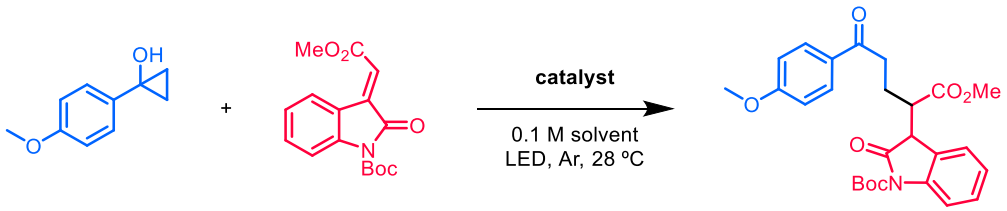

5
1.5 equiv

13
0.2 mmol

24

Entry	Catalyst	Solvent	Irradiation time, h	Wavelength, nm	NMR yield, %[b]	*ee*, %[c]	d.r.[c]
1	-	CH_2Cl_2	19	370	26	racemic	-
2	5 mol% **Sc(OTf)$_3$** 6 mol% ligand **L1**	CH_2Cl_2	22	370	17	10 / 14	1.4:1
3	10 mol% cat. **V**	CH_2Cl_2	22	370	21	13 / 0	1.8:1
4	10 mol% cat. **I**	CH_2Cl_2	22	370	24	10 / 3	1.6:1
5	20 mol% cat. **I**	CH_2Cl_2	20	370	26	13 / 19	1.2:1
6	1 mol% **TBADT** 20 mol% cat. **I**	CH_2Cl_2	20	370	48	6 / 10	1.2:1
7	20 mol% cat. **II**	CH_2Cl_2	20	370	18	13 / 22	1.3:1
8	20 mol% cat. **I**	CH_2Cl_2	22	395	39	13 / 12	1.4:1
9	20 mol% cat. **I**	$PhCH_3$	22	395	29	16 / 16	1.4:1

Table 2.[a] Reaction optimization in batch [a] Reaction conditions: alkene **13** (0.2 mmol), cyclopropanol **5** (1.5 equiv.), catalyst, solvent (0.1 M), LED, under Ar, 28 °C. [b] Yield was determined by ^{1}H NMR analysis of the crude reaction mixture against triphenylmethane as an internal standard. [c] *ee* and d.r. were determined by chiral HPLC analysis.

In summary, the addition of bifunctional hydrogen-bonding organocatalysts did not influence the yield of the reaction, which remained consistent for both alkenes employed. Notably, only the addition of TBADT resulted in a significant yield increase, nearly doubling it compared to organocatalyzed reactions. The structural composition of the alkene proved pivotal in determining enantioselectivity outcomes: while the reaction of benzylidene malononitrile **8** primarily yielded racemic products, oxindole **13** displayed moderate enantioselectivity. Utilizing Lewis acid catalysis with $Sc(OTf)_3$/PyBox ligand in the reaction of alkene **13** resulted in a lower yield compared to the control experiment (entry 1), albeit with similar enantioselectivity. Minimal enantioselectivity was achieved in the reaction of alkene **13** with the addition of catalysts **I** and **V**. Increasing the amount of organocatalyst **I** improved enantioselectivity, while yields remained unchanged. Altering the irradiation wavelength to 395 nm or using toluene as a solvent instead of dichloromethane did not significantly impact the results. The most favorable outcomes, obtained with alkene **13** and catalysts **I** and **II**, yielded approximately 25% NMR yield, up to 16% major diastereomer *ee*, 22% minor diastereomer *ee*, and a diastereomeric ratio of 1.6:1 for product **24**. We assume that enantioselectivity was low because the racemic reaction proceeded quickly even without an added catalyst, and the addition of the catalyst did not create a more favorable reaction pathway. We also speculate that the yield of the reactions, despite full conversion of starting materials, was low due to the formation of side products.

4. Conclusions

- Starting materials (cyclopropanol **5**, alkenes **8**, **10**, **13**, **15)** and the organocatalysts **20** and **22** were synthesised for the later use in photochemical reactions.
- The organocatalyzed photochemical reaction of electron-rich cyclopropanol and electron-deficient alkene was screened using cyclopropanol **5** and alkenes **8** and **13**, with the best results giving the yield of 25% and enantioselectivity of 16%/22%.
- It was observed that the enantioselectivity of the radical addition reactions via EDA complex formation depended on the structure of alkene used. Alkene **8** gave almost only racemic products, while usage of alkene **13** resulted in low enantioselectivities with all organocatalyzed reactions.
- Increasing the amount of organocatalyst **I** from 10 to 20 mol% slightly improved the enantioselectivity of the product **24**.

5. Experimental procedure

5.1 General information

^{1}H and ^{13}C spectra were recorded on a Bruker Avance III instrument at 400 MHz for ^{1}H and 100.6 MHz for ^{13}C. ^{1}H nuclear magnetic resonance (NMR) spectra are reported in parts per million (ppm) downfield relative to chloroform-*d* and methanol-d_4. High-performance liquid chromatography (HPLC) analyses were performed using Chiralpak AD-H and OD-H chiral columns. Precoated silica gel plates from Merck (DC-Kieselgel 60 F_{254}) were used for thin-layer chromatography (TLC) analysis. Flash column chromatography was performed on a Biotage® Isolera Prime with VWR Chemicals silica gel (0.040-0.063 mm). Commercial reagents were used as received.

5.2 Synthetic procedures for starting compounds and catalysts

5.2.1 Synthesis of 1-(4-methoxyphenyl)cyclopropan-1-ol (**5**)

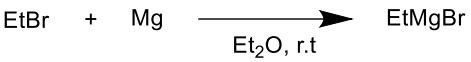

Magnesium turnings (23.5 mmol, 0.6 g, 1.0 equiv.) were added to a 50 mL 2-neck flask equipped with a condenser and the flask was filled with argon. An iodine crystal was then added and heated until sublimated to activate the magnesium. Ethyl bromide (25.9 mmol, 1.9 mL, 1.1 equiv.) solution in dry diethyl ether (16 mL) was added to the magnesium suspension at a controlled speed to maintain the mixture at reflux. When the exothermic reaction stopped, the reaction mixture was stirred for 10 additional minutes to obtain 1.5 M EtMgBr solution in Et_2O.

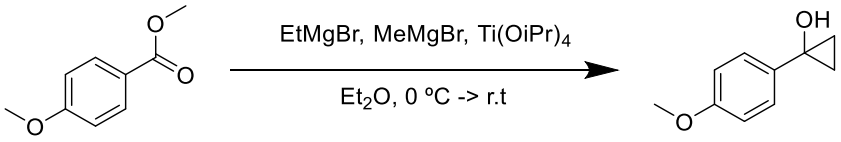

4 **5**

A 3 M solution of MeMgBr (22.5 mmol, 7.5 mL, 1.5 equiv.) in diethyl ether (7 mL) was added within 5 min by syringe to a solution of titanium isopropoxide (4.3 g, 1.0 equiv.) in dry diethyl ether (7 mL). The resulting yellow solution was cooled to 0 °C and methyl 4-methoxybenzoate **4** (15.0 mmol, 2.5 g, 1.0 equiv.) in diethyl ether (8 mL) was then added. A 1.5 M solution of EtMgBr (22.5 mmol, 15.0 mL, 1.5 equiv.) in diethyl ether (12 mL) was added over 30-40 min. The resulting reaction mixture was allowed to warm to room temperature, then stirred overnight. The reaction was then quenched at 0 °C by careful addition of cold 10% sulfuric acid solution (70 mL) and was extracted with diethyl ether (3 × 30 mL). The combined organic layers were washed with saturated sodium bicarbonate solution, brine and dried with magnesium sulfate. After the evaporation of solvent under reduced pressure, 1-(4-methoxyphenyl)cyclopropan-1-ol **5** (1.2 g, 49% yield) was isolated by flash column chromatography on silica gel (gradient of 2→40% diethyl ether/petroleum ether). ^{1}H NMR (400 MHz, $CDCl_3$) δ 7.26 (d, *J* = 8.8 Hz, 2H), 6.87 (d, *J* = 8.8 Hz, 2H), 3.80 (s, 3H), 2.50 (s, 1H), 1.26 – 1.14 (m, 2H), 1.04 – 0.91 (m, 2H). (Extra 1)

5.2.2 Synthesis of 2-benzylidenemalononitrile (**8**)

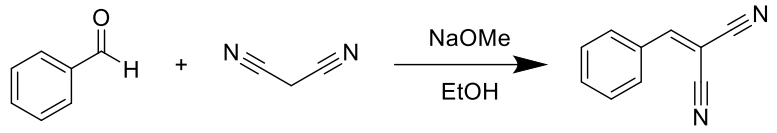

6 **7** **8**

A solution of benzaldehyde **6** (47 mmol, 4.8 mL, 1.0 equiv.) and malononitrile **7** (47 mmol, 3.1 g, 1.0 equiv.) in ethanol (240 mL) was treated with NaOMe (4.7 mmol, 0.3 g, 0.1 equiv.) portion wise, stirred at room temperature for 2 - 3 h, cooled to 0 °C in an ice bath, and filtered. The precipitate was washed with ethanol and the solvent was evaporated under reduced pressure to obtain the 2-benzylidenemalononitrile **8** (6.2 g, 85% yield). ^{1}H NMR (400 MHz, $CDCl_3$) δ 7.95 – 7.88 (m, 2H), 7.78 (s, 1H), 7.68 – 7.59 (m, 1H), 7.59 – 7.50 (m, 2H). (Extra 2)

5.2.3 Synthesis of (*E*)-3-benzylideneindolin-2-one (**10**)

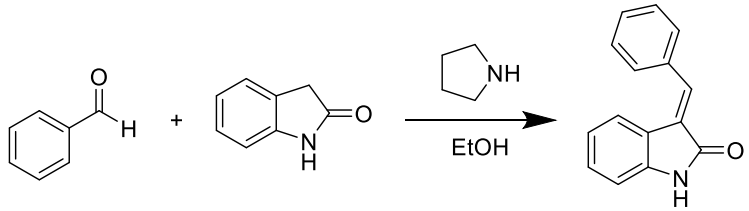

6 **9** **10**

A mixture of indolin-2-one **9** (4.7 mmol, 630 mg, 1.0 equiv.), benzaldehyde **6** (4.7 mmol, 500 mg, 1.0 equiv.) and pyrrolidine (0.50 mmol, 38 µL, 0.1 equiv.) in ethanol (16 mL) was heated to reflux for 2 hours and then quenched by water. A large amount of solid was precipitated, the filtered, and dried under high vacuum to obtain (*E*)-3-benzyleneindolin-2-one **10** (650 mg, 63% yield). The isolated product was determined to be the *E* isomer after comparing with the isolated *E* and *Z* isomer NMR spectra from the literature.[20] ^{1}H NMR (400 MHz, $CDCl_3$) δ 9.05 (s, 1H), 7.86 (s, 1H), 7.72 – 7.61 (m, 3H), 7.52 – 7.41 (m, 3H), 7.22 (td, *J* = 7.7, 1.2 Hz, 1H), 6.96 – 6.92 (m, 1H), 6.87 (td, *J* = 7.7, 1.1 Hz, 1H). (Extra 3)

5.2.4 Synthesis of *tert*-butyl (*E*)-3-(2-methoxy-2-oxoethylidene)-2-oxoindoline-1-carboxylate (**12**)

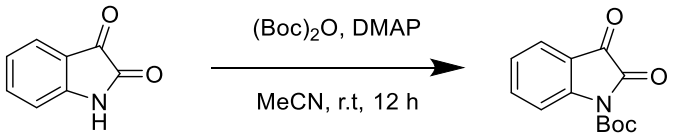

11 **12**

Commercially available isatin **11** (8.0 mmol, 1.2 g, 1.0 equiv.) was dissolved in acetonitrile (40 mL) and cooled to 0 °C. To this solution were added 4-(dimethylamino)pyridine (DMAP) (0.8 mmol, 0.1 g, 0.10 equiv.) and di-*tert*-butyl decarbonate ($(Boc)_2O$) (9.6 mmol, 2.1 g, 1.2 equiv.) and the mixture was stirred at room temperature for 12 h. The reaction mixture was then cooled to 0 °C and quenched with saturated aqueous ammonium chloride. The aqueous layer was extracted with ethyl acetate, the combined organic layers were washed with 0.5 M hydrochloric acid solution and saturated solution of

sodium bicarbonate and then dried over sodium sulfate. After the removal of solvent, the crude was purified by flash column chromatography on silica gel (gradient of 2→25% ethyl acetate/petroleum ether) to obtain the product N-Boc-protected isatin **12** (0.6 g, 31% yield).

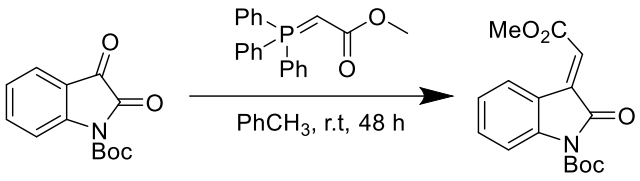

12 **13**

A solution of *tert*-butyl 2,3-dioxoindoline-1-carboxylate **12** (2.4 mmol, 0.61 g, 1.0 equiv.) and phosphonium ylide (2.7 mmol, 0.89 g, 1.1 equiv.) in toluene (8 mL) was stirred at room temperature for 48 hours. The solvent was evaporated under vacuum and crude product was purified by flash column chromatography on silica gel (gradient of 2→15% ethyl acetate/petroleum ether) to obtain *tert*-butyl (*E*)-3-(2-methoxy-2-oxoethylidene)-2-oxoindoline-1-carboxylate **13** (0.51 g, 70% yield). ^{1}H NMR (400 MHz, $CDCl_3$) δ 8.69 (dd, *J* = 7.8, 1.4 Hz, 1H), 7.92 (dt, *J* = 8.3, 0.9 Hz, 1H), 7.44 (ddd, *J* = 8.4, 7.6, 1.4 Hz, 1H), 7.20 (td, *J* = 7.7, 1.1 Hz, 1H), 6.92 (s, 1H), 3.88 (s, 3H), 1.65 (s, 9H). (Extra 4)

5.2.5 Synthesis of 4-(2,2-difluorovinyl)benzonitrile (**15**)

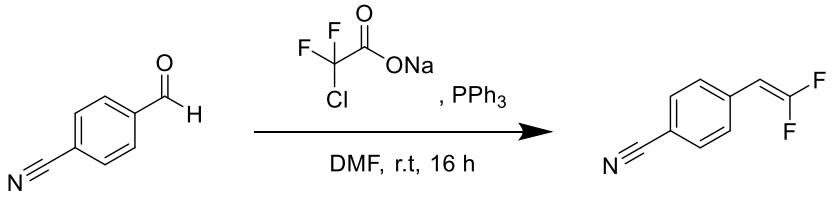

14 **15**

To a solution of 4-formylbenzonitrile **14** (7.0 mmol, 0.92 g, 1.0 equiv.) and triphenyl phosphine (PPh_3) (8.4 mmol, 2.2 0g, 1.2 equiv.) in dimethylformamide (14 mL) was added sodium chlorodifluoroacetate (14 mmol, 2.13 g, 2.0 equiv.) and the mixture stirred at room temperature for 16 hours. After the aldehyde was consumed completely, water was added to the reaction slowly and the mixture was extracted with aqueous 5% solution of lithium chloride and then a 1:1 mix of petroleum ether and diethylether. The combined organic layer was dried over sodium sulfate, filtrated, and concentrated under reduced pressure. The residue was purified by column chromatography on silica gel (gradient of 2→10% ethyl acetate/petroleum ether) to obtain 4-(2,2-difluorovinyl)benzonitrile **15** (0.48 g, 40% yield). ^{1}H NMR (400 MHz, $CDCl_3$) δ 7.64 – 7.59 (m, 2H), 7.45 – 7.39 (m, 2H), 5.33 (dd, *J* = 25.6, 3.4 Hz, 1H). (Extra 5)

5.2.6 Synthesis of 9-amino(9-deoxy)epihydroquinine (18)

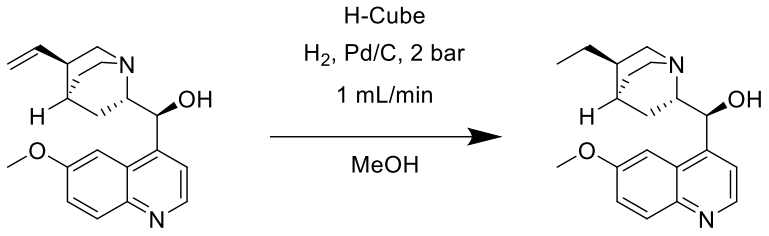

16 17

9-amino(9-deoxy)epihydroquinine **18** was synthesized according to a procedure reported in the literature[19]. Compound **16** (6.0 mmol, 1.95 g, 1.0 equiv.) was dissolved in methanol (110 mL) and then hydrogenated in the H-Cube® at a pressure of 2 bar and with a flow rate of 1 mL/min to obtain (1*S*)-((4*S*,5*R*)-5-ethylquinuclidin-2-yl)(6-methoxyquinolin-4-yl)methanol **17** (1.46 g, 75% yield). ^{1}H NMR (400 MHz, $CDCl_3$) δ 8.79 – 8.63 (m, 1H), 8.00 (d, *J* = 9.2 Hz, 1H), 7.52 (d, *J* = 4.5 Hz, 1H), 7.34 (dd, *J* = 9.2, 2.7 Hz, 1H), 7.25 (s, 1H), 5.55 (s, 1H), 3.91 (s, 3H), 3.51 – 3.25 (m, 1H), 3.15 (q, *J* = 8.9 Hz, 1H), 3.08 (dd, *J* = 13.5, 9.9 Hz, 1H), 2.95 (s, 1H), 2.73 – 2.55 (m, 1H), 2.40 (d, *J* = 13.5 Hz, 1H), 1.84 – 1.76 (m, 1H), 1.76 – 1.59 (m, 2H), 1.58 – 1.48 (m, 1H), 1.49 – 1.37 (m, 2H), 1.33 – 1.18 (m, 2H), 0.82 (t, *J* = 7.3 Hz, 3H). (Extra 6)

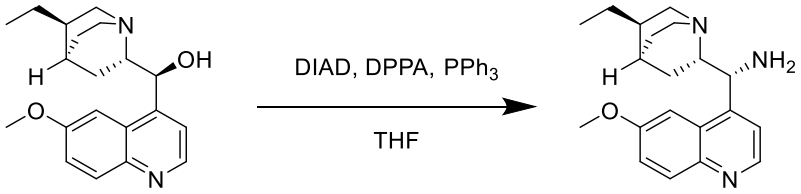

17 18

To (1*S*)-((4*S*,5*R*)-5-ethylquinuclidin-2-yl)(6-methoxyquinolin-4-yl)methanol **17** (4.5 mmol, 1.5 g, 1.0 equiv.) was added half of the PPh_3 (2.7 mmol, 0.7 g, 0.60 equiv.). The air was evacuated under vacuum and the flask was refilled with argon gas three times. Anhydrous tetrahydrofuran (18 mL) was added to the flask with a syringe and stirred until the solid completely dissolved. The reaction mixture was cooled down to 0 °C using a water-ice bath and stirred for a further 5 min. Diisopropyl azodicarboxylate (DIAD) (5.4 mmol, 1.1 mL, 1.2 equiv.) was slowly added with a syringe to the cold solution during 5 minutes. 5 minutes after the addition, diphenylphosphoryl azide (DPPA) (5.4 mmol, 1.2 mL, 1.2 equiv.) was added dropwise for 15 minutes and the mixture was stirred for a further 15 minutes at 0 °C. After stirring, the cooling bath was removed, and the mixture was allowed to warm up to room temperature. The mixture was stirred for 2.5 h at room temperature during which it became a yellowish suspension. Then the mixture is heated to 50 °C and stirred for a further 2 h, during which it became homogenous again. The rest of the PPh_3 (2.7 mmol, 0.70 g, 0.60 equiv.) was added to the solution. The mixture was then stirred overnight at 50 °C. Water (3.5 mL) was added to the mixture. The mixture was then stirred for 4 h at 45 °C and overnight at room temperature.

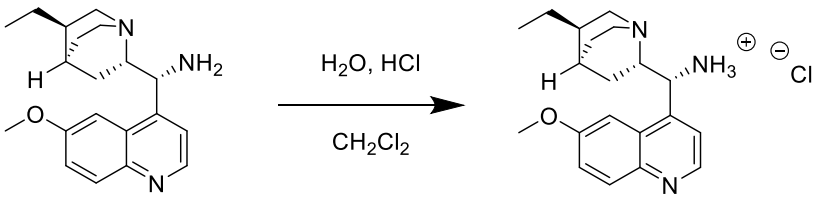

18 **25**

The mixture was transferred to a round-bottom flask using dichloromethane and solvents were then removed under reduced pressure. Dichloromethane (22 mL) was added to the mixture, which was then stirred until homogenous. 2 M aqueous hydrochloric acid solution (22 mL) was slowly added to the mixture while stirring vigorously for 10 minutes. Then the mixture was extracted with dichloromethane and solvents were removed under reduced pressure to obtain a bright yellow solid. To purify the hydrochloride salt via recrystallization, it was dissolved in a minimum amount of methanol (5.5 mL) to fully dissolve it while heating the mixture to reflux. Ethyl acetate (2.4 mL) was slowly added until the opalescence of the mixture becomes persistent. The flask was allowed to cool down to room temperature before being refrigerated to 0-4 °C. Overnight, recrystallization was allowed to take place. The mixture was filtrated to separate the solid crystals, which were then washed by ethyl acetate previously cooled to 5-10 °C using an ice bath. The solvent in the mother liquid was removed under reduced pressure and the recrystallization was performed using methanol (5 mL) and ethyl acetate (2 mL). The solid was then dried under reduced pressure to obtain (1*R*)-((2*S*,4*S*,5*R*)-5-ethylquinuclidin-2-yl)(6-methoxyquinolin-4-yl)methanaminium chloride **25** (1.1 g, 59% yield). ^{1}H NMR (400 MHz, CD_3OD) δ 9.22 (d, *J* = 5.8 Hz, 1H), 8.63 (d, *J* = 5.8 Hz, 1H), 8.34 (d, *J* = 9.4 Hz, 1H), 8.20 – 8.06 (m, 1H), 7.96 (dd, *J* = 9.4, 2.5 Hz, 1H), 6.12 (d, *J* = 10.5 Hz, 1H), 4.41 – 4.25 (m, 1H), 4.23 (s, 3H), 3.83 (dd, *J* = 12.9, 10.4 Hz, 1H), 3.58 – 3.45 (m, 1H), 3.41 – 3.32 (m, 1H), 2.16 – 1.82 (m, 6H), 1.72 – 1.45 (m, 2H), 1.09 (dd, *J* = 13.8, 8.0 Hz, 1H), 0.94 (t, *J* = 7.4 Hz, 3H). (Extra 7)

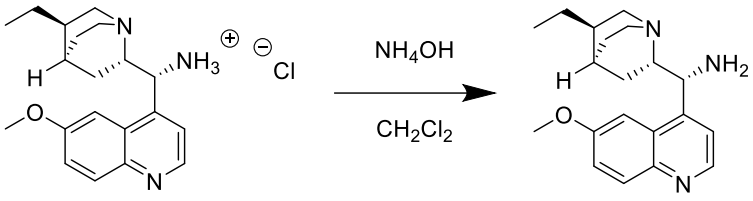

25 **18**

Previously obtained (1*R*)-((2*S*,4*S*,5*R*)-5-ethylquinuclidin-2-yl)(6-methoxyquinolin-4-yl)methanaminium chloride **25** (3.0 mmol, 1.1 g, 1.0 equiv.) was dissolved in dichloromethane (7 mL). While stirring the mixture, 5 M aqueous solution of ammonium hydroxide (4 mL) was added slowly and stirred vigorously for 5 min. The aqueous layer was extracted with dichloromethane, the combined organic layers were dried with sodium sulfate and the solvent was removed under reduced pressure to obtain 9-amino(9-deoxy)epihydroquinine **18** (0.80 g, 80% yield). ^{1}H NMR (400 MHz, $CDCl_3$) δ 8.75 (d, *J* = 4.5 Hz, 1H), 8.03 (d, *J* = 9.2 Hz, 1H), 7.65 (s, 1H), 7.47 (d, *J* = 4.6 Hz, 1H), 7.38 (dd, *J* = 9.2, 2.7 Hz, 1H), 4.59 (d, *J* = 10.2 Hz, 1H), 3.97 (s, 3H), 3.34 – 3.13 (m, 2H), 3.10 – 2.98 (m, 1H), 2.78 (ddd, *J* = 14.8, 10.4, 5.2 Hz, 1H), 2.52 (ddd, *J* = 13.6, 4.8, 2.5 Hz, 1H), 1.66 – 1.19 (m, 7H), 0.82 (t, *J* = 7.3 Hz, 3H), 0.74 (ddt, *J* = 13.7, 7.5, 1.8 Hz, 1H). (Extra 8)

5.2.7 Synthesis of 3-((3,5-bis(trifluoromethyl)phenyl)amino)-4-(((1*R*)-((4*S*,5*R*)-5-ethylquinuclidin-2-yl)(6-methoxyquinolin-4-yl)methyl)amino)cyclobut-3-ene-1,2-dione (20)

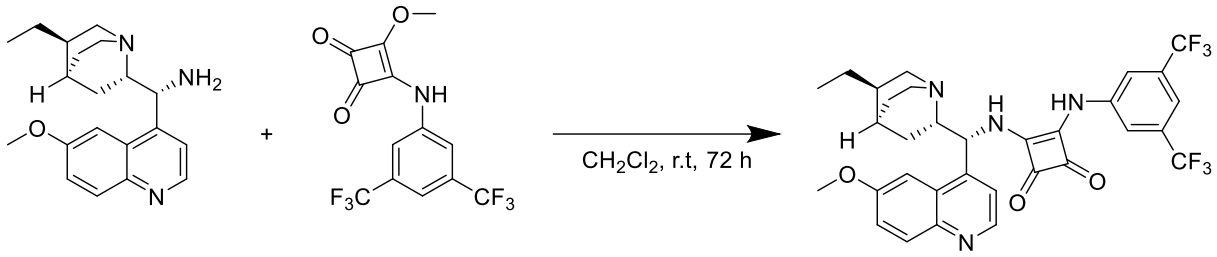

18 **19** **20**

To a stirred solution of 9-amino(9-deoxy)epihydroquinine **18** (1.1 mmol, 360 mg, 1.0 equiv.) in dichloromethane (13 mL) was added 3-((3,5-bis(trifluoromethyl)phenyl)amino)-4-methoxycyclobut-3-ene-1,2-dione **19** (1.1 mmol, 360 mg, 1.1 equiv). After stirring for 72 h, the solvent was evaporated and the crude reaction mixture was purified by flash column chromatography on silica gel (gradient of 10→100% acetonitrile/H_2O) to obtain 3-((3,5-bis(trifluoromethyl)phenyl)amino)-4-(((1*R*)-((2*S*,4*S*,5*R*)-5-ethylquinuclidin-2-yl)(6-methoxyquinolin-4-yl)methyl)amino)cyclobut-3-ene-1,2-dione **20** (540 mg, 81% yield). ^{1}H NMR (400 MHz, CD_3OD) δ 8.75 (d, *J* = 4.7 Hz, 1H), 8.03 – 7.93 (m, 3H), 7.90 (s, 1H), 7.66 (d, *J* = 4.7 Hz, 1H), 7.49 (s, 1H), 7.46 (dd, *J* = 9.3, 2.6 Hz, 1H), 6.31 (d, *J* = 11.0 Hz, 1H), 4.02 (s, 3H), 3.59 (q, *J* = 9.2 Hz, 2H), 2.84 – 2.71 (m, 1H), 2.61 (dd, *J* = 14.0, 3.6 Hz, 1H), 1.74 – 1.51 (m, 6H), 1.50 – 1.36 (m, 2H), 0.90 (t, *J* = 7.3 Hz, 3H), 0.72 (dd, *J* = 13.5, 7.2 Hz, 1H). (Extra 9)

5.2.8 Synthesis of 1-(3,5-bis(trifluoromethyl)phenyl)-3-((1*R*)-((4*S*,5*R*)-5-ethylquinuclidin-2-yl)(6-methoxyquinolin-4-yl)methyl)thiourea (22)

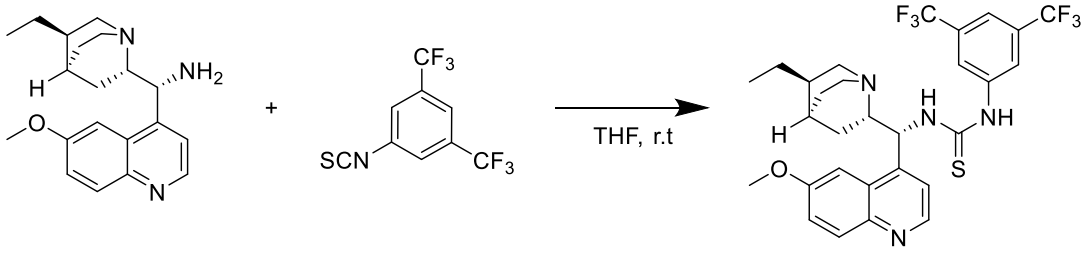

18 **21** **22**

To a solution of 9-amino(9-deoxy)epihydroquinine **18** (1.3 mmol, 430 mg, 1.0 equiv.) in dry tetrahydrofuran (4.0 mL) was slowly added a solution of 3,5-bis(trifluoromethyl)phenyl isothiocyanate **21** (1.3 mmol, 240 µL, 1.0 equiv.) in 2 mL of dry tetrahydrofuran at ambient temperature. The mixture was stirred overnight, and the solvent was removed in vacuo. The residue was purified by flash column chromatography on silica gel (gradient of 20→100% acetonitrile/H_2O) to obtain 1-(3,5-bis(trifluoromethyl)phenyl)-3-((1*R*)-((2*S*,4*S*,5*R*)-5-ethylquinuclidin-2-yl)(6-methoxyquinolin-4-yl)methyl)thiourea **22** (260 mg, 33% yield). ^{1}H NMR (400 MHz,CD_3OD) δ 8.69 (d, *J* = 4.8 Hz, 1H), 8.10 (d, *J* = 1.8 Hz, 3H), 7.95 (d, *J* = 9.2 Hz, 1H), 7.62 – 7.59 (m, 1H), 7.58 (d, *J* = 4.8 Hz, 1H), 7.46 (dd, *J* = 9.2, 2.7 Hz, 1H), 6.36 (d, *J* = 11.2 Hz, 1H), 4.03 (s, 3H), 3.60 (t, *J* = 13.7 Hz, 1H), 3.40 (q, *J* = 9.5 Hz, 1H), 2.93 – 2.72 (m, 1H), 2.53 (ddd, *J* = 13.5, 5.2, 2.4 Hz, 1H), 1.83 – 1.67 (m, 1H), 1.67 – 1.47 (m, 3H), 1.37 (dddd, *J* = 20.8, 19.1, 13.7, 8.4 Hz, 3H), 0.86 (t, *J* = 7.3 Hz, 3H), 0.84 (s, 1H). (Extra 10)

5.3 General procedure and setup of the photochemical reactions.

5.3.1 Photochemical batch reaction setup

All photochemical experiments at 370 nm were carried out in 10 mL Schlenk tubes placed into a 3D printed reactor designed by Noël group[21] (Reactor A) and irradiated with a Kessil PR160 43 W 370 nm lamp (Figure 4). A computer fan was attached to the bottom of the reactor for cooling. The intensity of the light was regulated to 100% for each reaction, but could be regulated (25, 50 or 75%) differently. All photochemical experiments at 395 nm were carried out in 10 mL Schlenk tubes placed into a custom reactor (Reactor B) and irradiated by a 395 nm UV-LED strip (Figure 4). Air was blown into the reactor via a tube for cooling.

5.3.2 General procedure for organocatalyzed photochemical reactions.

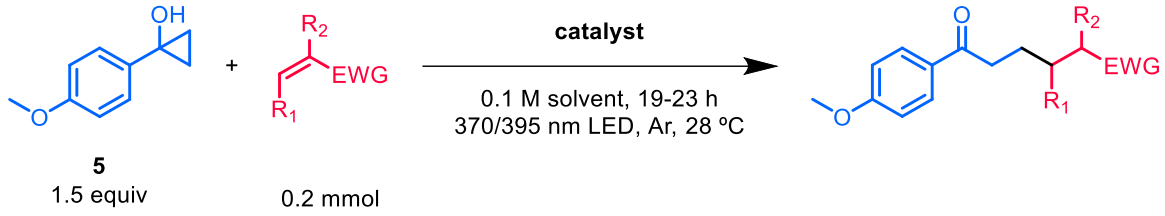

In an oven-dried 10 mL Schlenk tube equipped with a stirring bar, alkene (0.2 mmol), cyclopropanol **5** (0.3 mmol, 1.5 equiv.) and catalyst were dissolved in the solvent (1 mL, 0.1 M). The tube was capped, and the reaction mixture was degassed three times via three cycles of freeze-pump-thaw and then back-filled with argon gas. The Schlenk tube was then placed in the reactor and irradiated at 370 or 395 nm for 19–23 h at ambient temperature. After the completion of the reaction, the solvents were removed by evaporation. The NMR of crude reaction mixture was measured against triphenylmethane as standard.

5.3.3 Procedures for HPLC analysis

Crude reaction mixture and product was separated using a TLC plate with petroleum ether:ethyl acetate 2:1 as an eluent. TLC silica gel containing product was scraped off the TLC plate into an Eppendorf and the solid was extracted with a 2:1 mixture of *n*-hexane:*i*-propanol and filtered. 20 µL of the filtrate was injected into the HPLC with the following methods:

- HPLC conditions for the compound 2-(4-(4-methoxyphenyl)-4-oxo-1-phenylbutyl)malononitrile **23**: Chiralpak AD-H, *n*-hexane:*i*-propanol 8:2, flow rate 1.0 ml/min, 25 °C, λ = 210 nm.
- HPLC conditions for the compound tert-butyl 3-(1-methoxy-5-(4-methoxyphenyl)-1,5-dioxopentan-2-yl)-2-oxoindoline-1-carboxylate **24**: Chiralpak OD-H, *n*-hexane:*i*-propanol 9:1, flow rate 1.5 ml/min, 35 °C, λ = 254 nm.

Acknowledgements

First and foremost, I would like to thank my supervisor Anastasiya Krech for their guidance in both practical and theoretical work and their patience with me while writing this thesis.

Next, I thank Assistant Professor Maksim Ošeka for his teachings and help in polishing this work.

I also thank all the students and workers of the organic chemistry department for their cooperation.

6. References

(1) Anastas, P. T.; Warner, J. C. *Green Chemistry: Theory and Practice*; Oxford University Press, 2000. https://doi.org/10.1093/oso/9780198506980.001.0001.

(2) Krech, A.; Yakimchyk, V.; Jarg, T.; Kananovich, D.; Ošeka, M. Ring-Opening Coupling Reaction of Cyclopropanols with Electrophilic Alkenes Enabled by Decatungstate as Photoredox Catalyst. *Adv. Synth. Catal.* **2024**, *366* (1), 91–100. https://doi.org/10.1002/adsc.202300939.

(3) Braslavsky, S. E. Glossary of Terms Used in Photochemistry, 3rd Edition (IUPAC Recommendations 2006). *Pure Appl. Chem.* **2007**, *79* (3), 293–465. https://doi.org/10.1351/pac200779030293.

(4) Roth, H. D. The Beginnings of Organic Photochemistry. *Angew. Chem. Int. Ed. Engl.* **1989**, *28* (9), 1193–1207. https://doi.org/10.1002/anie.198911931.

(5) Albini, A.; Dichiarante, V. The 'Belle Époque' of Photochemistry. *Photochem. Photobiol. Sci.* **2009**, *8* (2), 248–254. https://doi.org/10.1039/b806756b.

(6) Muller, P. Glossary of Terms Used in Physical Organic Chemistry (IUPAC Recommendations 1994). *Pure Appl. Chem.* **1994**, *66* (5), 1077–1184. https://doi.org/10.1351/pac199466051077.

(7) Goti, G.; Manal, K.; Sivaguru, J.; Dell'Amico, L. The Impact of UV Light on Synthetic Photochemistry and Photocatalysis. *Nat. Chem.* **2024**, *16*, 684–692. https://doi.org/10.1038/s41557-024-01472-6.

(8) Prier, C. K.; Rankic, D. A.; MacMillan, D. W. C. Visible Light Photoredox Catalysis with Transition Metal Complexes: Applications in Organic Synthesis. *Chem. Rev.* **2013**, *113* (7), 5322–5363. https://doi.org/10.1021/cr300503r.

(9) Crisenza, G. E. M.; Mazzarella, D.; Melchiorre, P. Synthetic Methods Driven by the Photoactivity of Electron Donor–Acceptor Complexes. *J. Am. Chem. Soc.* **2020**, *142* (12), 5461–5476. https://doi.org/10.1021/jacs.0c01416.

(10) Lima, C. G. S.; de M. Lima, T.; Duarte, M.; Jurberg, I. D.; Paixão, M. W. Organic Synthesis Enabled by Light-Irradiation of EDA Complexes: Theoretical Background and Synthetic Applications. *ACS Catal.* **2016**, *6* (3), 1389–1407. https://doi.org/10.1021/acscatal.5b02386.

(11) Arceo, E.; Jurberg, I. D.; Álvarez-Fernández, A.; Melchiorre, P. Photochemical Activity of a Key Donor–Acceptor Complex Can Drive Stereoselective Catalytic α-Alkylation of Aldehydes. *Nat. Chem.* **2013**, *5* (9), 750–756. https://doi.org/10.1038/nchem.1727.

(12) Hong, B.-C.; Indurmuddam, R. R. Tetrabutylammonium Decatungstate (TBADT), a Compelling and Trailblazing Catalyst for Visible-Light-Induced Organic Photocatalysis. *Org. Biomol. Chem.* **2024**, *22* (19), 3799–3842. https://doi.org/10.1039/D4OB00171K.

(13) Dondi, D.; Fagnoni, M.; Albini, A. Tetrabutylammonium Decatungstate-Photosensitized Alkylation of Electrophilic Alkenes: Convenient Functionalization of Aliphatic C-H Bonds. *Chem. – Eur. J.* **2006**, *12* (15), 4153–4163. https://doi.org/10.1002/chem.200501216.

(14) Zheng, Z.; Hill, C. L. Alkanes to Nitriles and α-Iminoesters. Polyoxotungstate Photocatalytic Radical Chain Initiation. *Chem. Commun.* **1998**, *34* (22), 2467–2468. https://doi.org/10.1039/A805036H.

(15) Waele, V. D.; Poizat, O.; Fagnoni, M.; Bagno, A.; Ravelli, D. Unraveling the Key Features of the Reactive State of Decatungstate Anion in Hydrogen Atom Transfer (HAT) Photocatalysis. *ACS Catal.* **2016**, *6* (10), 7174–7182. https://doi.org/10.1021/acscatal.6b01984.

(16) Hegedus, L. S. Organocatalysis in Organic Synthesis. *J. Am. Chem. Soc.* **2009**, *131* (50), 17995–17997. https://doi.org/10.1021/ja908581u.

(17) Fang, X.; Wang, C.-J. Recent Advances in Asymmetric Organocatalysis Mediated by Bifunctional Amine–Thioureas Bearing Multiple Hydrogen-Bonding Donors. *Chem. Commun.* **2015**, *51* (7), 1185–1197. https://doi.org/10.1039/C4CC07909D.

(18) Kulinkovich, O. G.; Kananovich, D. G. Advanced Procedure for the Preparation of Cis-1,2-Dialkylcyclopropanols – Modified Ate Complex Mechanism for Titanium-Mediated Cyclopropanation of Carboxylic Esters with Grignard Reagents. *Eur. J. Org. Chem.* **2007**, *2007* (13), 2121–2132. https://doi.org/10.1002/ejoc.200601035.

(19) Cassani, C.; Martín-Rapún, R.; Arceo, E.; Bravo, F.; Melchiorre, P. Synthesis of 9-Amino(9-Deoxy)Epi Cinchona Alkaloids, General Chiral Organocatalysts for the Stereoselective Functionalization of Carbonyl Compounds. *Nat. Protoc.* **2013**, *8* (2), 325–344. https://doi.org/10.1038/nprot.2012.155.
(20) Park, J. H.; Kim, E.; Chung, Y. K. Heterobimetallic Cobalt/Rhodium Nanoparticle-Catalyzed Carbonylative Cycloaddition of 2-Alkynylanilines to Oxindoles. *Org. Lett.* **2008**, *10* (21), 4719–4721. https://doi.org/10.1021/ol801978n.
(21) Noël, T.; Zysman-Colman, E. The Promise and Pitfalls of Photocatalysis for Organic Synthesis. *Chem Catal.* **2022**, *2* (3), 468–476. https://doi.org/10.1016/j.checat.2021.12.015.

Abstract

Many molecules abundantly found in nature are chiral and can be easily used as building blocks for chiral reagents. Their abundance makes these reagents ecologically friendly, which is why it is important to develop chemistry that leverages them. The development of enantioselective reactions is crucial for various fields, such as pharmacology and agrochemical manufacturing, because enantiomers of molecules often have different effects. The more enantioselective the reaction, the greener it is, since less purification is required, thereby reducing waste. Combining photochemistry with asymmetric synthesis is another step towards greener chemistry due to the benefits and efficiency of light irradiation compared to traditional thermal reactions.

The main objective of this work was to optimize the asymmetric photochemical reaction of electron-rich cyclopropanols and electron-deficient alkenes proceeding via EDA complex formation, with the aim of inducing enantioselectivity through the addition of an organocatalyst.

For this work, several starting compounds and organocatalysts were synthesized with low to high yields. Two different electron-poor alkenes were used as substrates for photochemical reaction optimization and five different bifunctional organocatalysts were used as additives among some different reagents. The best results for optimization of the reaction were a 29% yield with enantioselectivities of 16% for the major diastereomer and 22% for the minor diastereomer and a diastereomeric ratio of 1.6:1. The results of the asymmetric photochemical reaction optimization - showing low yields and low enantioselectivities - indicate that there is still significant optimization needed before the commercial use of such a reaction is feasible.

Annotatsioon

Paljud looduses ohtralt leiduvad molekulid on kiraalsed ning neid on kerge kasutada kiraalsete reagentide alustena. Molekulide rohkus teeb need ökoloogiliselt sõbralikuks ehk roheliseks, mistõttu on tähtis arendada keemiat, mis selliseid molekule kasutab. Enantioselektiivsete reaktsioonide arendamine on üliloluline valdkondades nagu farmakoloogia ja agrokeemiatööstus, kuna molekulide enantiomeeridel võivad tihti olla erinevad mõjud. Mida suurem enantioselektiivsus, seda rohelisem on reaktsioon, sest vähem puhastamist on vaja teostada ja seega tekib jäätmeid vähem. Fotokeemia kombineerimine asümmeetrilise sünteesiga on järgmine samm rohelisema keemia poole tänu valgusega indutseeritud reaktsioonide eelistele ja tõhususele võrreldes harilike soojusega aktiveeritud reaktsioonidega.

Selle töö peamine eesmärk oli asümmeetrilise fotokeemilise reaktsiooni optimeerimine, mis toimub elektron-rikaste tsüklopropanoolide ja elektron-vaeste alkeenide vahel tänu elektron doonor-aktseptor (EDA) kompleksile, ja enantioselektiivsuse saavutamine reaktsioonis läbi organokatalüsaatori lisamise.

Mitu lähtereagenti ja organokatalüsaatorit sünteesiti selle töö raames, saavutades nii madalaid kui kõrgeid saagiseid. Kahte erinevat electron-vaest alkeeni kasutati substraatidena fotokeemilise reaktsiooni optimeerimiseks ning viite erinevat organokatalüsaatorit kasutati lisanditena peale mõne teise reagendi. Parimad tulemused reaktsiooni optimeerimisele olid 29% saagis, 16% peamise diastereomeeri enantioselektiivsus, 22% väiksema diastereomeeri enantioselektiivsus ja 1.6:1 diastereomeerne suhe. Asümmeetrilise fotokeemilise reaktsiooni optimeerimise tulemused – madalad saagised ja enantioselektiivused – näitavad, et veel on vaja märkimisväärselt palju optimeerimist läbi viia, enne kui sellise reaktsiooni kaubanduslik kasutus on teostatav.

Extras

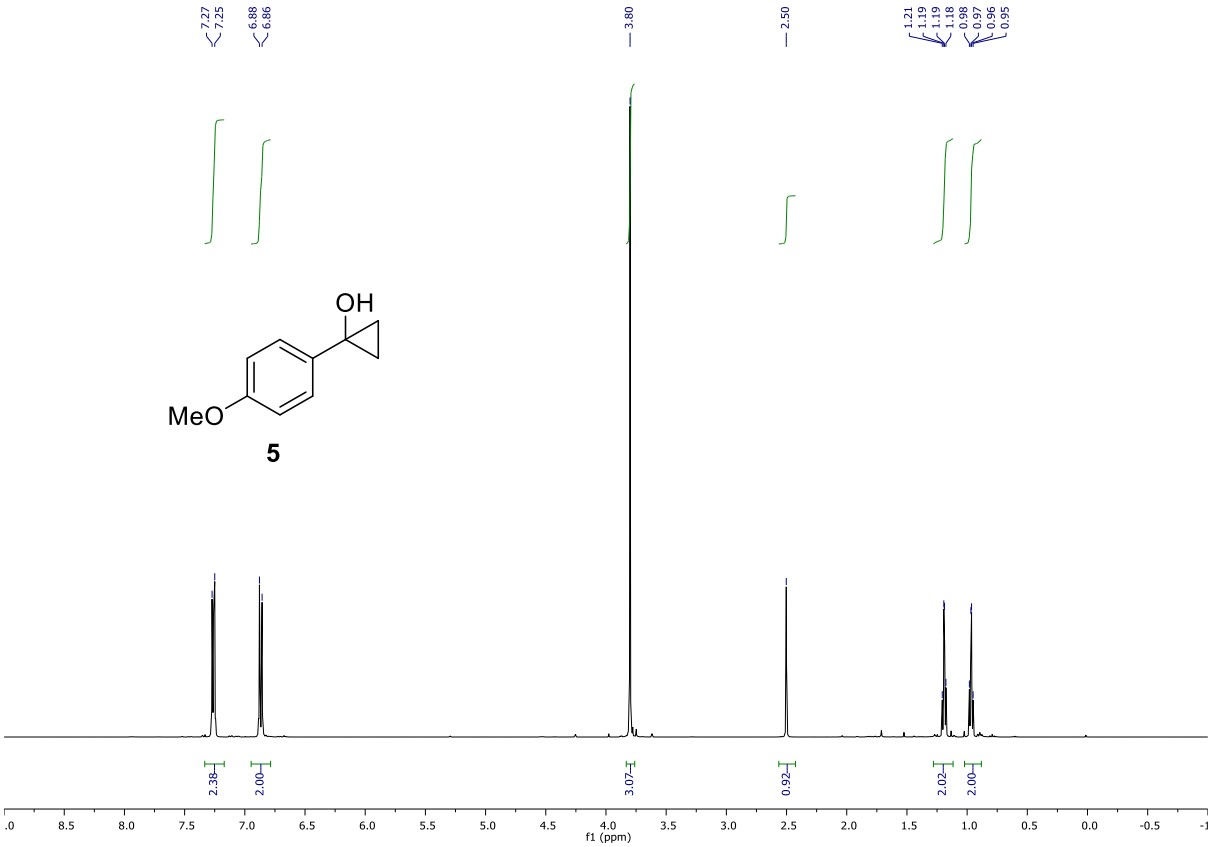

Extra 1. ^{1}H NMR of **5** (400 MHz, $CDCl_3$).

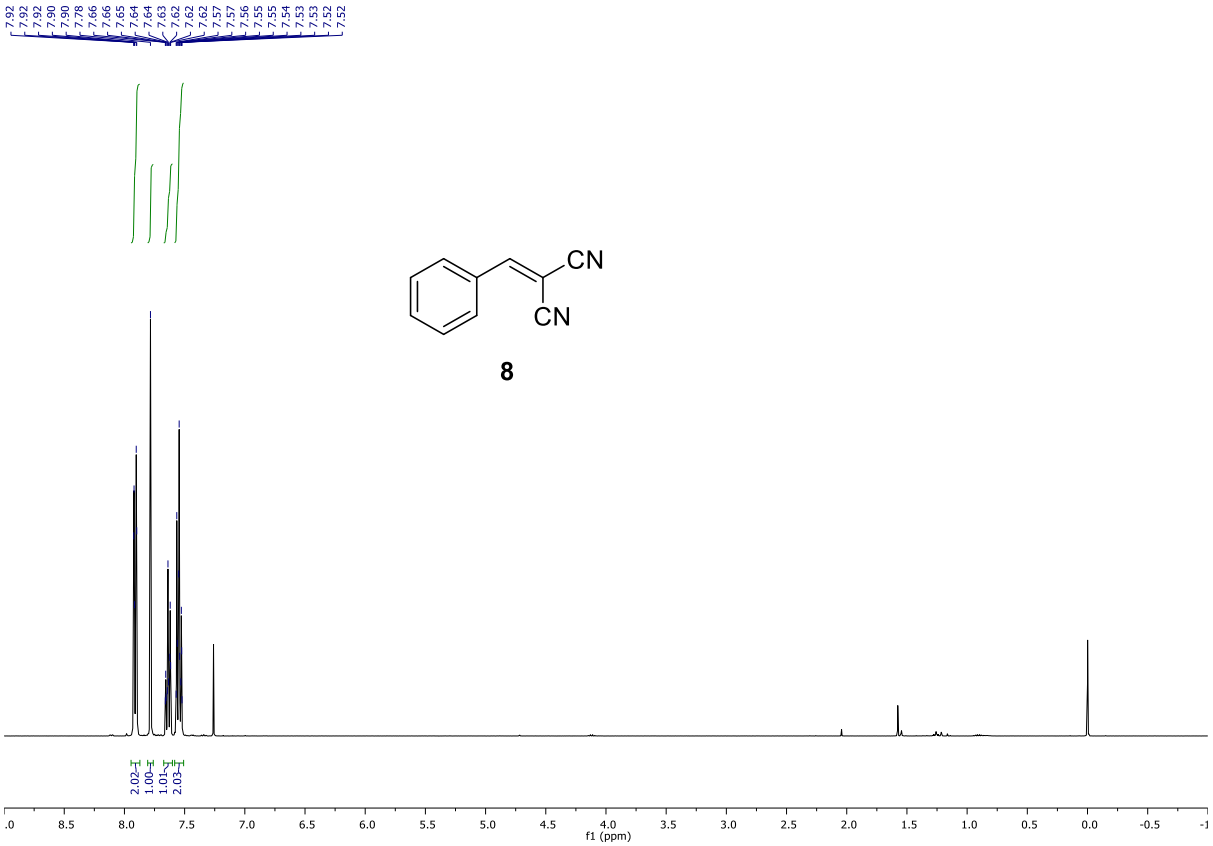

Extra 2. ^{1}H NMR of **8** (400 MHz, $CDCl_3$).

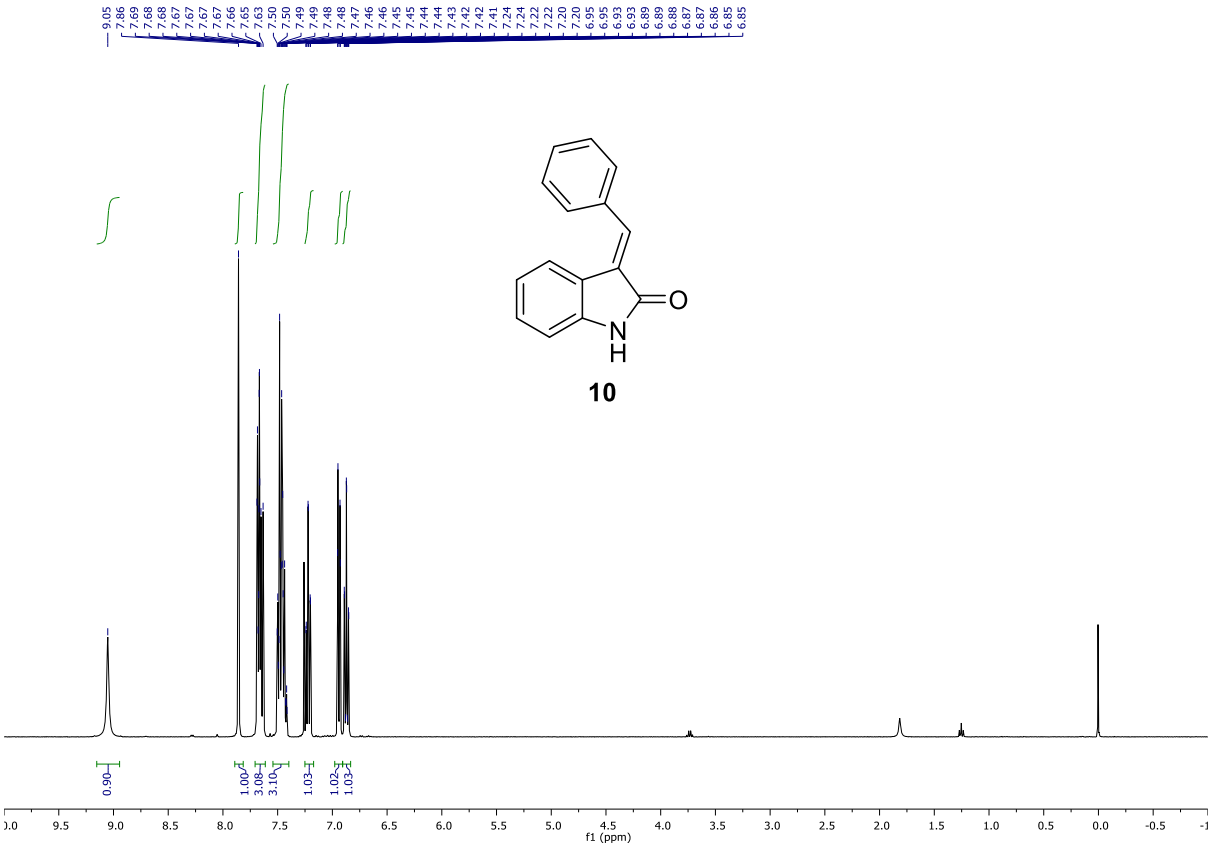

Extra 3. ^{1}H NMR of **10** (400 MHz, $CDCl_3$).

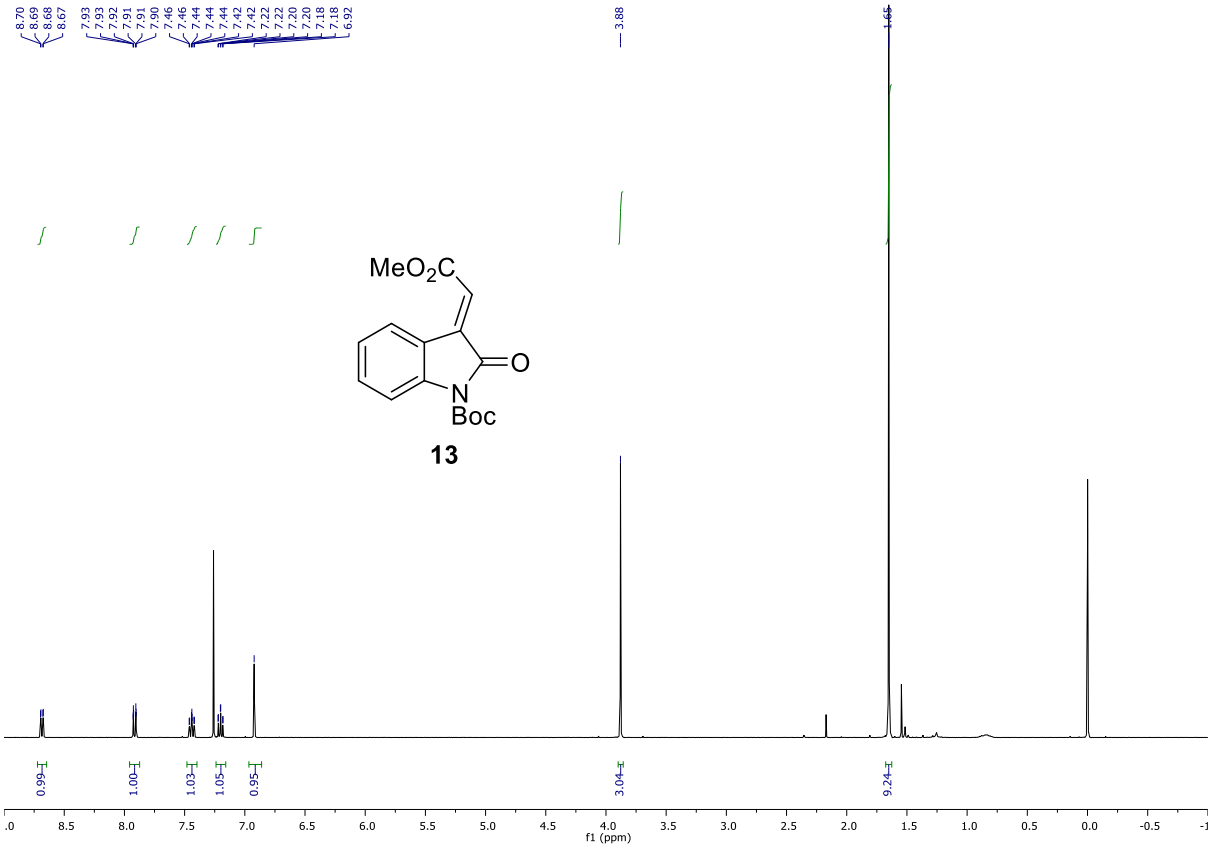

Extra 4. ^{1}H NMR of **13** (400 MHz, $CDCl_3$).

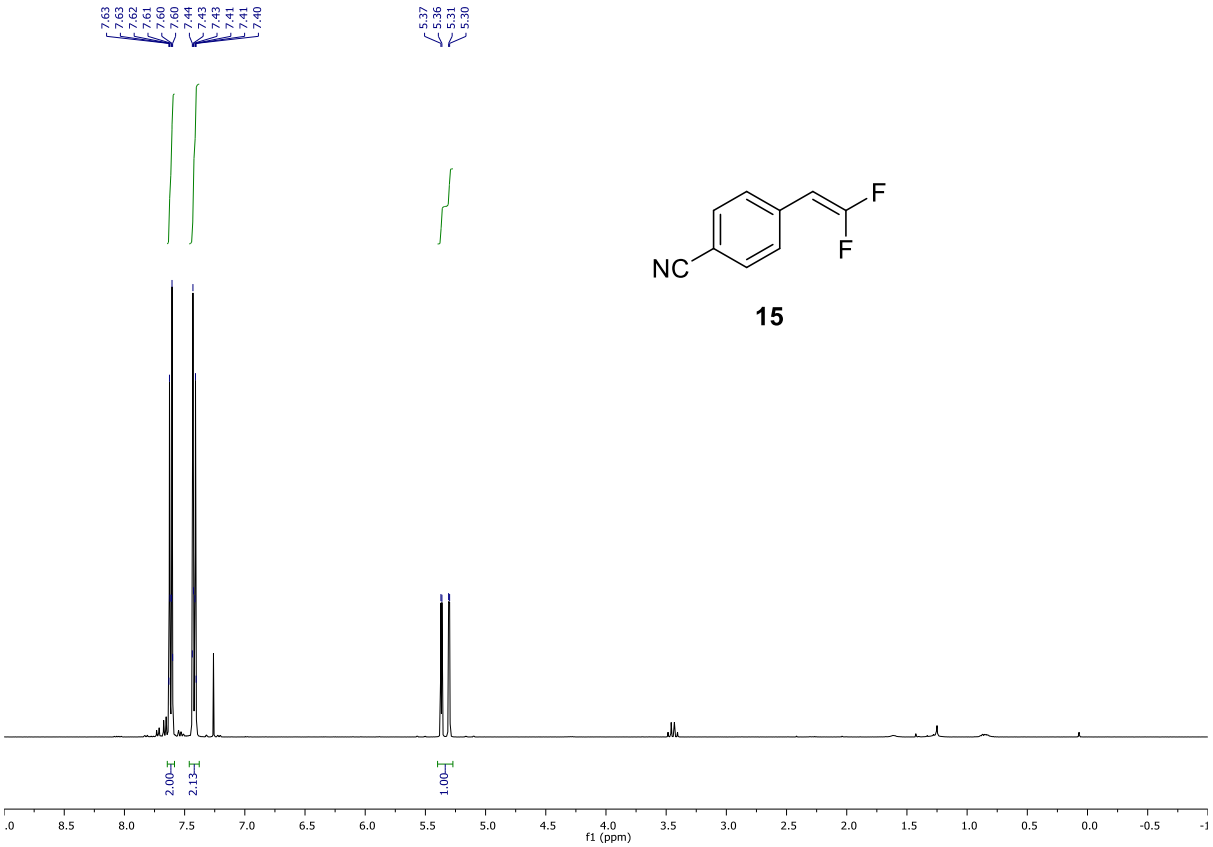

Extra 5. ^{1}H NMR of **15** (400 MHz, $CDCl_3$).

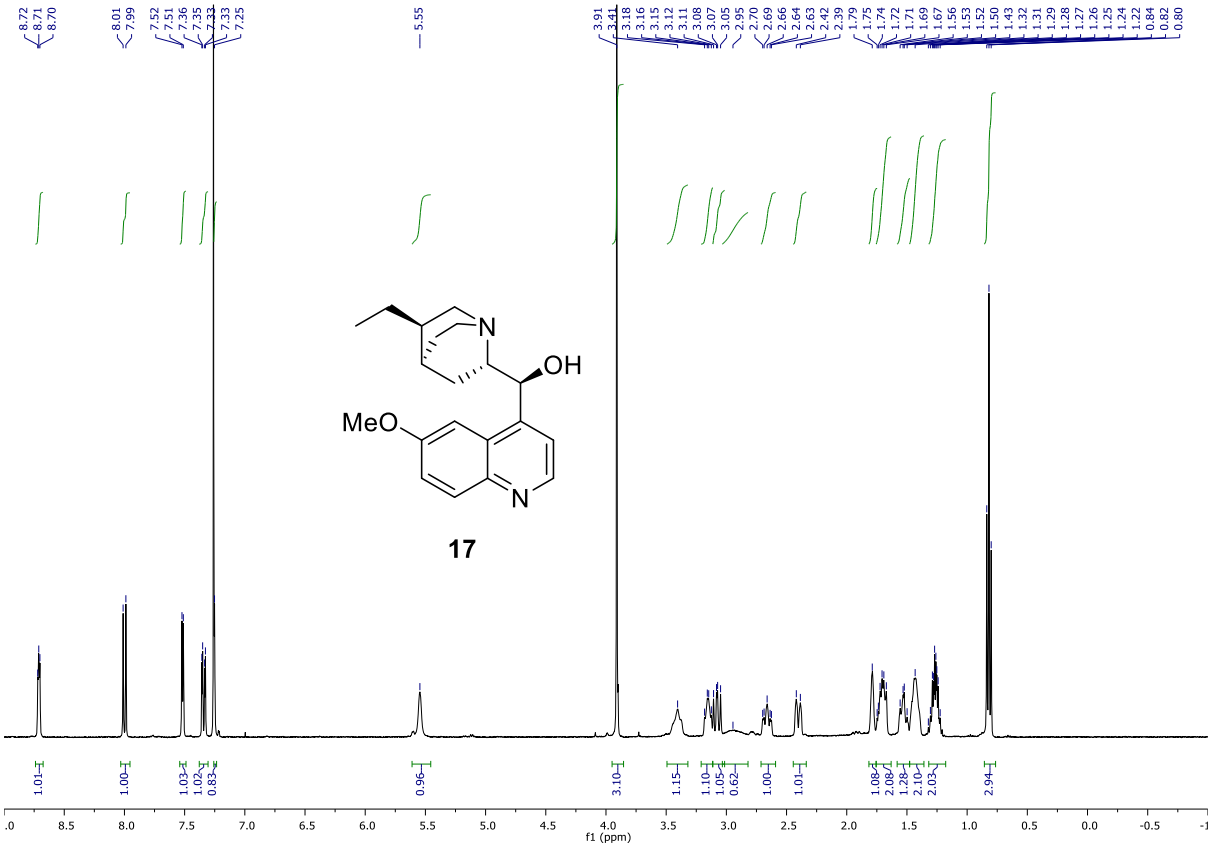

Extra 6. ^{1}H NMR of **17** (400 MHz, $CDCl_3$).

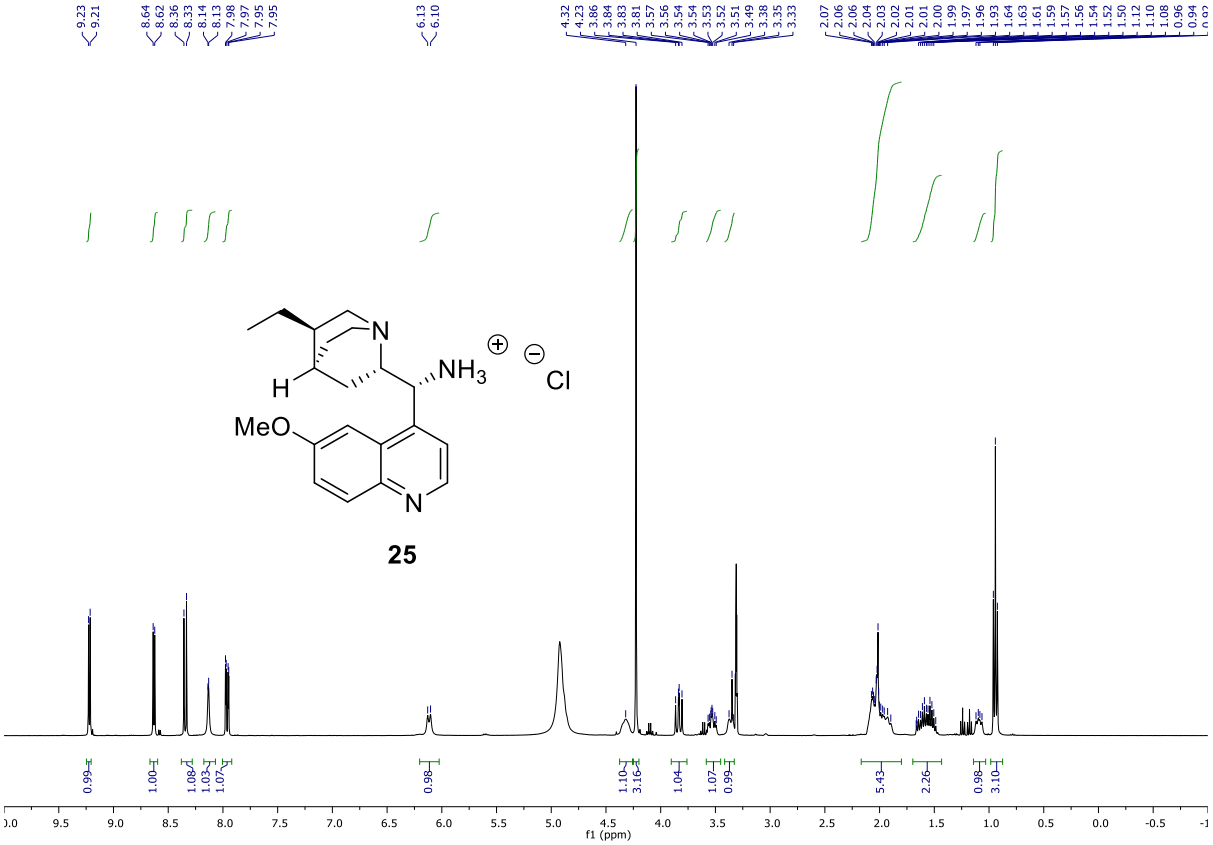

Extra 7. ^{1}H NMR of **25** (400 MHz, CD_3OD).

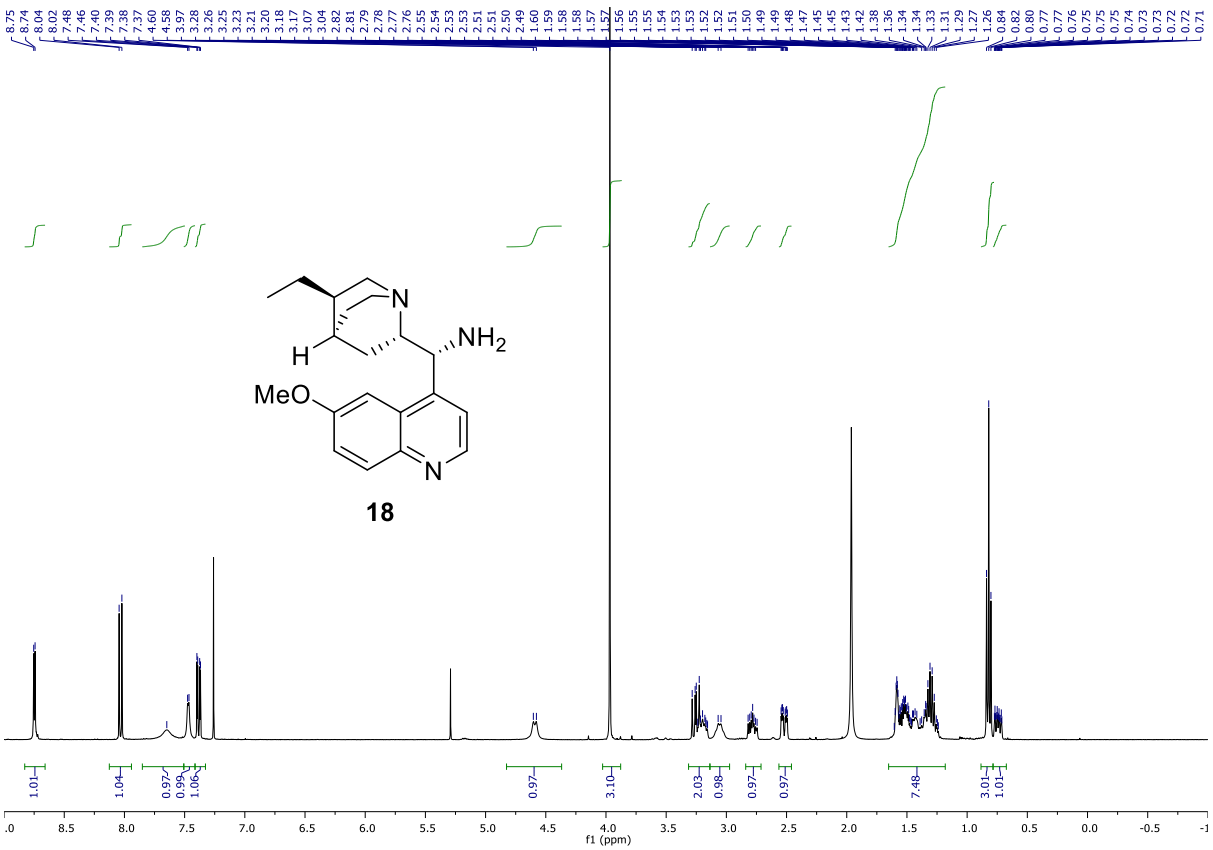

Extra 8. ^{1}H NMR of **18** (400 MHz, $CDCl_3$).

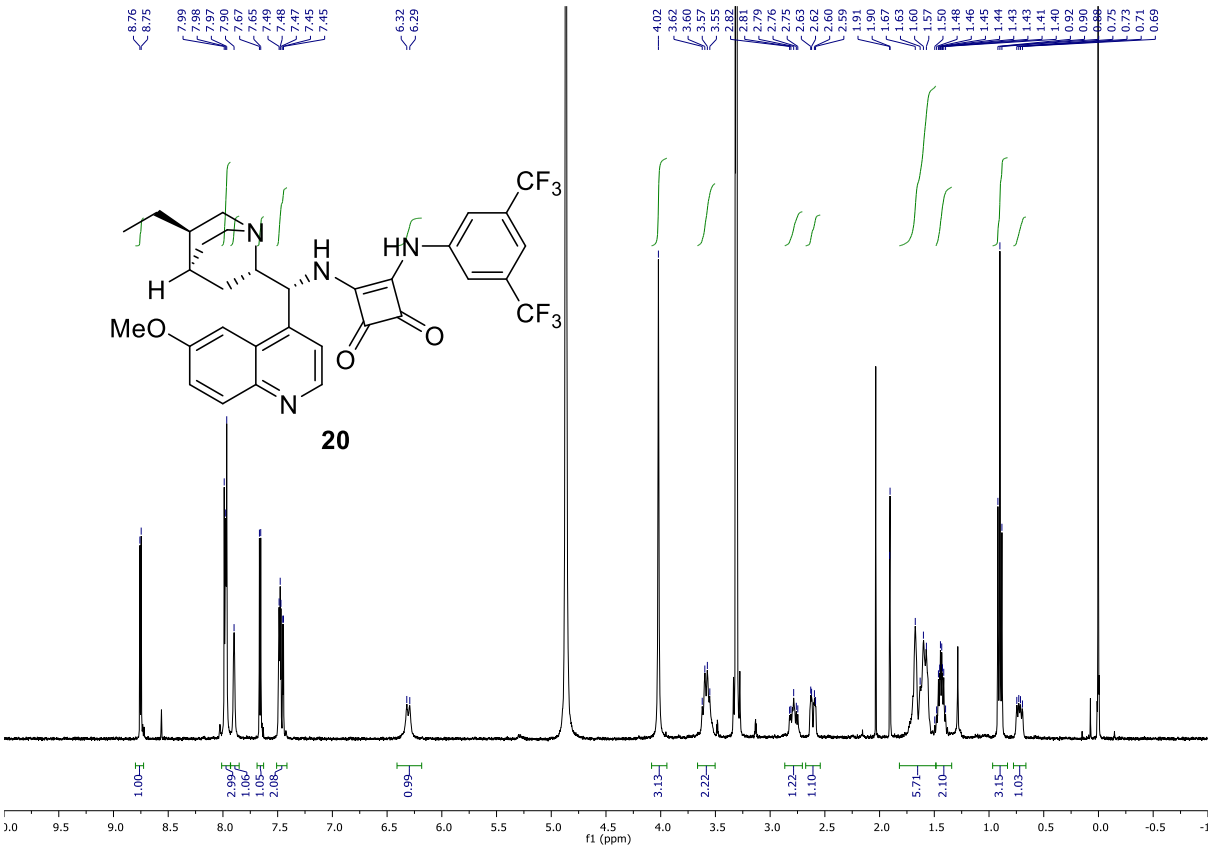

Extra 9. ^{1}H NMR of **20** (400 MHz, CD_3OD).

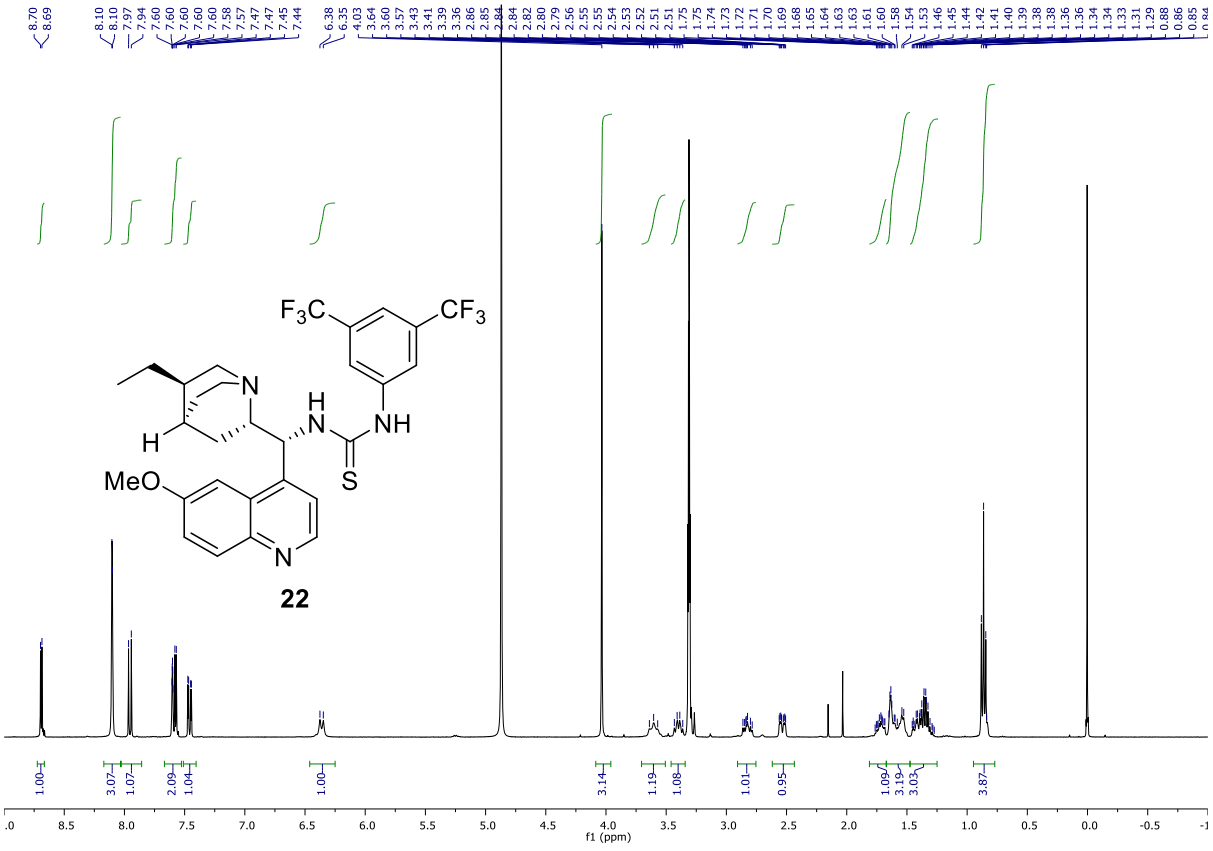

Extra 10. ^{1}H NMR of **22** (400 MHz, CD_3OD).

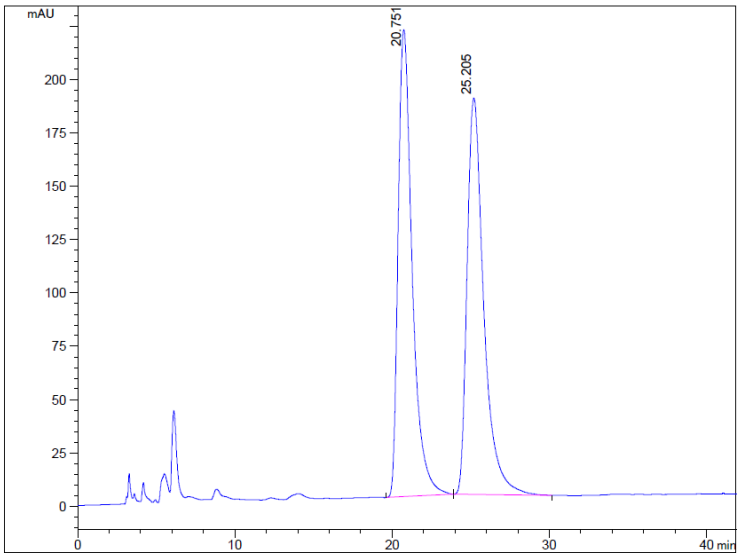

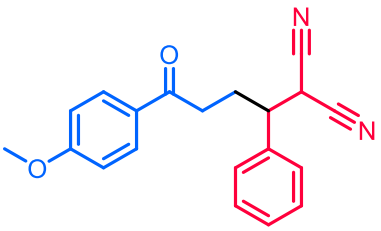

23

Signal 1: VWD1 A, Wavelength=210 nm

Peak #	RT [min]	Type	Width [min]	Area	Area %	Name
1	20.751	BB	0.945	13595.146	49.804	
2	25.205	BB	1.116	13702.226	50.196	

Extra 11. The HPLC chromatogram of racemic **23**.

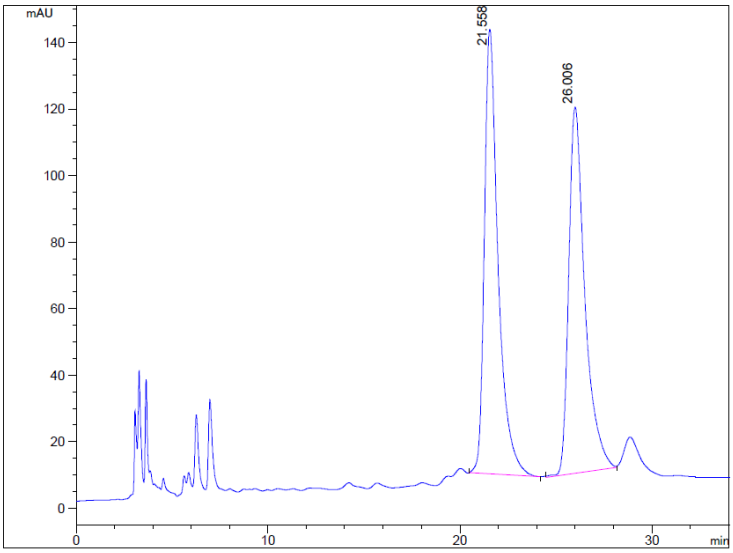

Signal 1: VWD1 A, Wavelength=210 nm

Peak #	RT [min]	Type	Width [min]	Area	Area %	Name
1	21.558	MM	0.826	6620.646	50.681	
2	26.006	MM	0.975	6442.835	49.319	

Extra 12. The HPLC chromatogram of **23** for Table 1, entry 1.

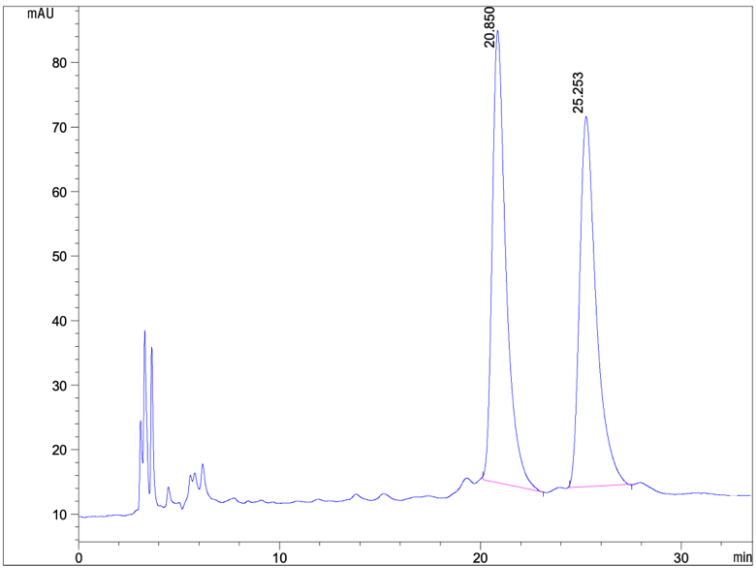

Signal 1: VWD1 A, Wavelength=210 nm

Peak #	RT [min]	Type	Width [min]	Area	Area %	Name
1	20.850	MM	0.800	3361.204	50.537	
2	25.253	MM	0.957	3289.718	49.463	

Extra 13. The HPLC chromatogram of **23** for Table 1, entry 2.

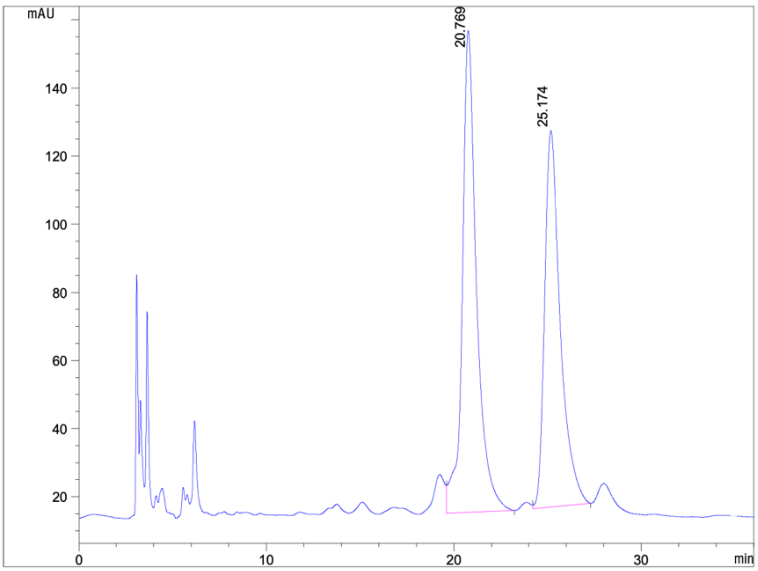

Signal 1: VWD1 A, Wavelength=210 nm

Peak #	RT [min]	Type	Width [min]	Area	Area %	Name
1	20.769	VB	0.765	7474.136	53.712	
2	25.174	VB	0.869	6441.178	46.288	

Extra 14. The HPLC chromatogram of **23** for Table 1, entry 3.

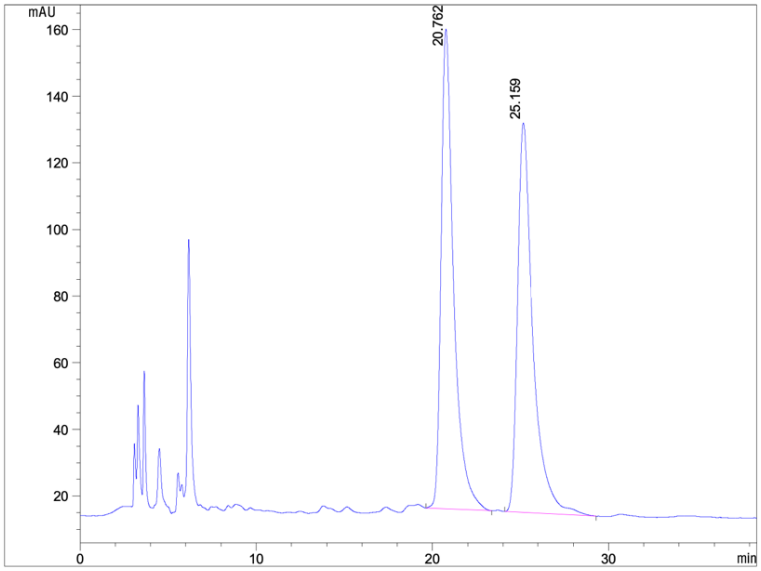

Signal 1: VWD1 A, Wavelength=210 nm

Peak #	RT [min]	Type	Width [min]	Area	Area %	Name
1	20.762	BB	0.726	7132.161	50.004	
2	25.159	BB	0.894	7131.142	49.996	

Extra 15. The HPLC chromatogram of **23** for Table 1, entry 4.

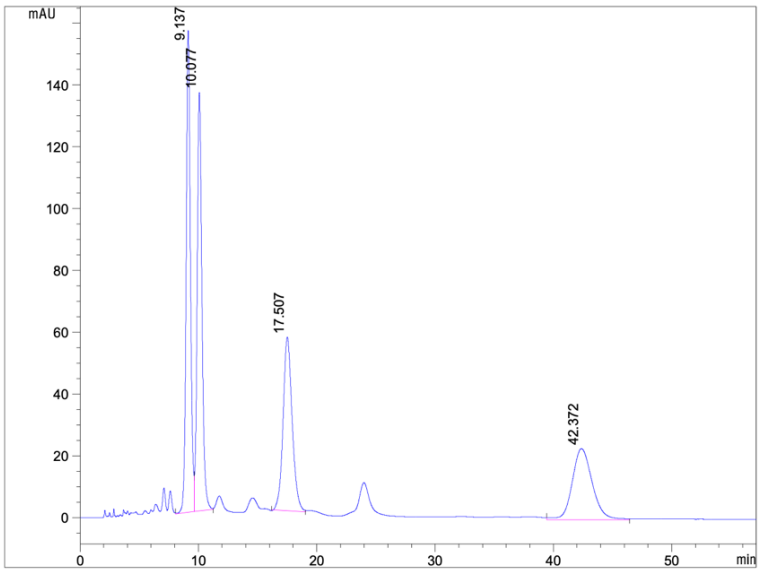

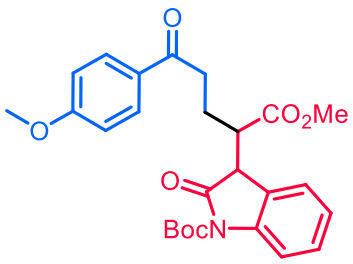

24

Signal 1: VWD1 A, Wavelength=254 nm

Peak #	RT [min]	Type	Width [min]	Area	Area %	Name
1	9.137	MF	0.418	3912.226	29.162	
2	10.077	FM	0.465	3776.147	28.148	
3	17.507	MM	0.890	2997.842	22.346	
4	42.372	MM	1.971	2729.132	20.343	

Extra 16. The HPLC chromatogram of racemic **24**.

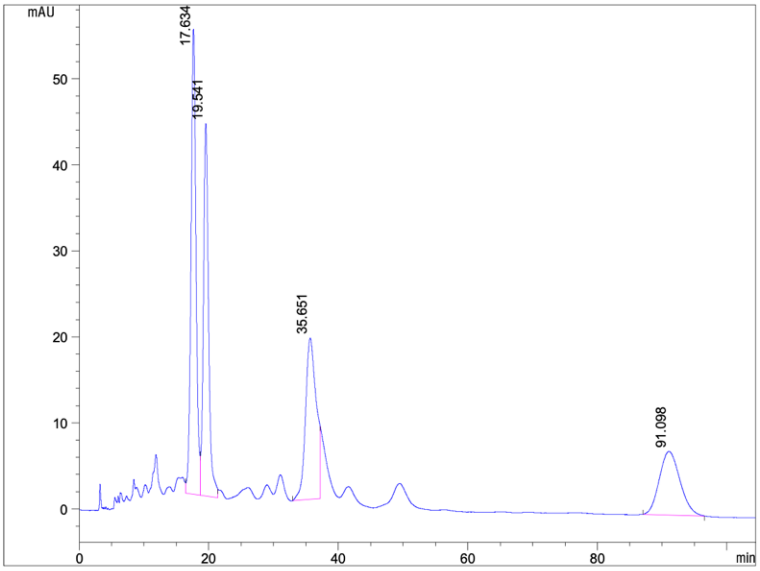

Signal 1: VWD1 A, Wavelength=254 nm

Peak #	RT [min]	Type	Width [min]	Area	Area %	Name
1	17.634	MF	0.893	2895.611	31.890	
2	19.541	MF	0.917	2382.409	26.238	
3	35.651	MF	1.921	2164.142	23.834	
4	91.098	BB	2.599	1637.749	18.037	

Extra 17. The HPLC chromatogram of **24** for Table 2, entry 2.

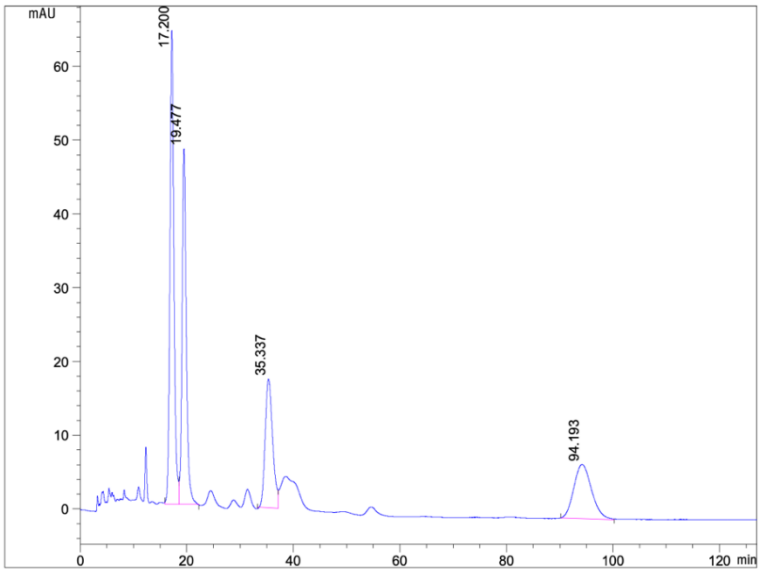

Signal 1: VWD1 A, Wavelength=254 nm

Peak #	RT [min]	Type	Width [min]	Area	Area %	Name
1	17.200	MF	0.884	3409.032	36.034	
2	19.477	FM	0.912	2636.286	27.866	
3	35.337	MF	1.634	1709.152	18.066	
4	94.193	MM	3.862	1706.143	18.034	

Extra 18. The HPLC chromatogram of **24** for Table 2, entry 3.

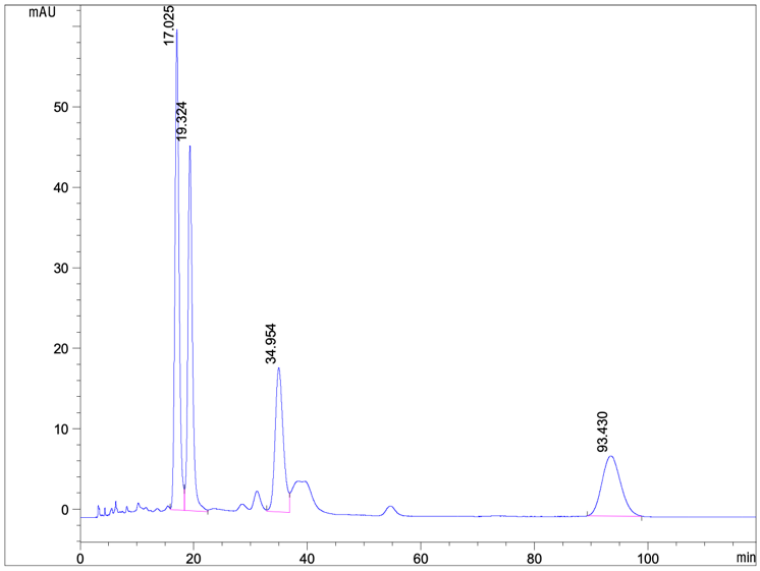

Signal 1: VWD1 A, Wavelength=254 nm

Peak #	RT [min]	Type	Width [min]	Area	Area %	Name
1	17.025	MF	0.855	3063.184	33.791	
2	19.324	FM	0.926	2520.234	27.801	
3	34.954	MF	1.658	1783.682	19.676	
4	93.430	BB	2.670	1698.058	18.732	

Extra 19. The HPLC chromatogram of **24** for Table 2, entry 4.

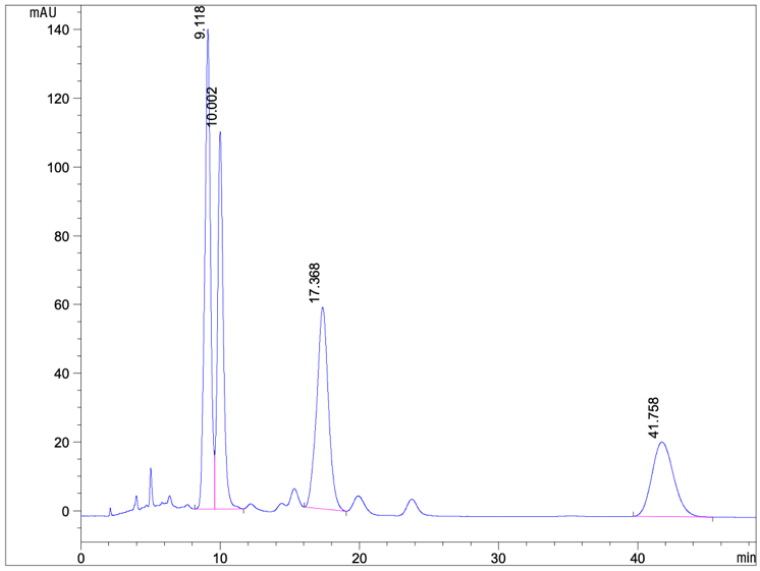

Signal 1: VWD1 A, Wavelength=254 nm

Peak #	RT [min]	Type	Width [min]	Area	Area %	Name
1	9.118	BV	0.425	4054.873	31.251	
2	10.002	VB	0.430	3131.639	24.136	
3	17.368	BB	0.879	3443.356	26.538	
4	41.758	MM	1.802	2345.169	18.074	

Extra 20. The HPLC chromatogram of **24** for Table 2, entry 5.

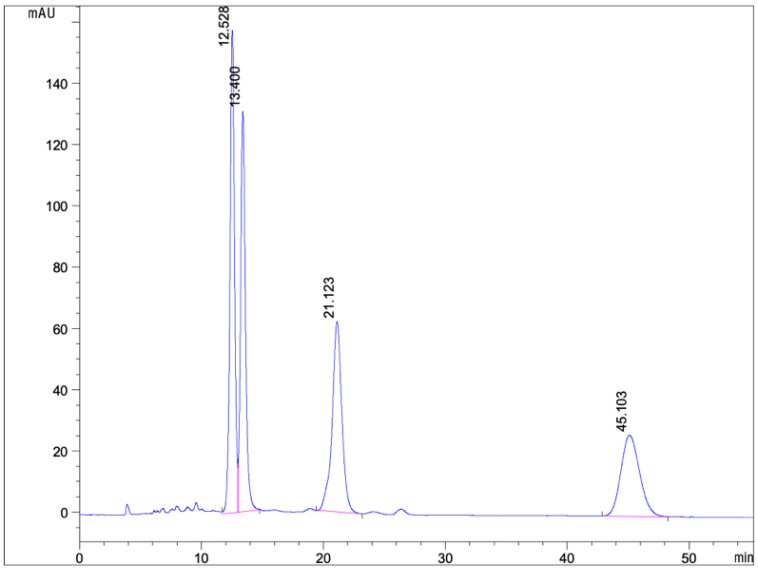

Signal 1: VWD1 A, Wavelength=254 nm

Peak #	RT [min]	Type	Width [min]	Area	Area %	Name
1	12.528	MF	0.437	4128.700	29.451	
2	13.400	FM	0.463	3626.431	25.868	
3	21.123	MM	0.926	3453.054	24.631	
4	45.103	BB	1.540	2810.759	20.050	

Extra 21. The HPLC chromatogram of **24** for Table 2, entry 6

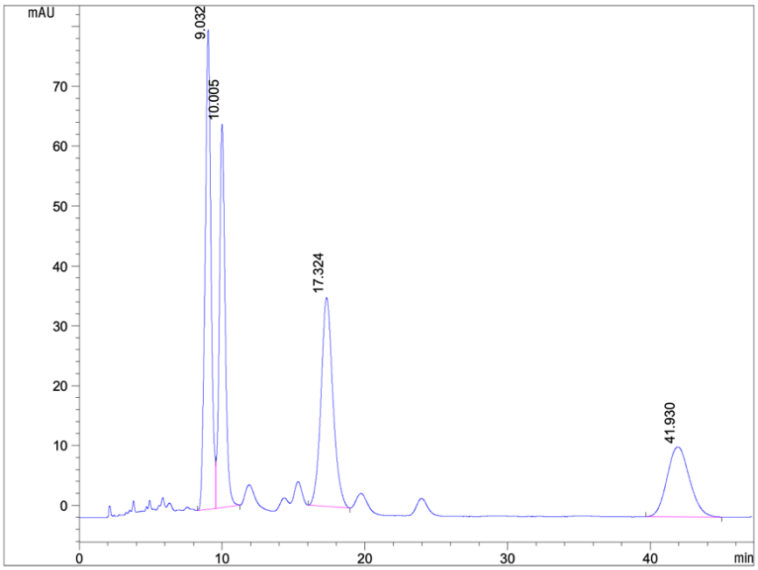

Signal 1: VWD1 A, Wavelength=254 nm

Peak #	RT [min]	Type	Width [min]	Area	Area %	Name
1	9.032	BV	0.427	2325.408	31.282	
2	10.005	VB	0.429	1807.799	24.319	
3	17.324	BB	0.872	2019.278	27.164	
4	41.930	BB	1.452	1281.223	17.235	

Extra 22. The HPLC chromatogram of **24** for Table 2, entry 7.

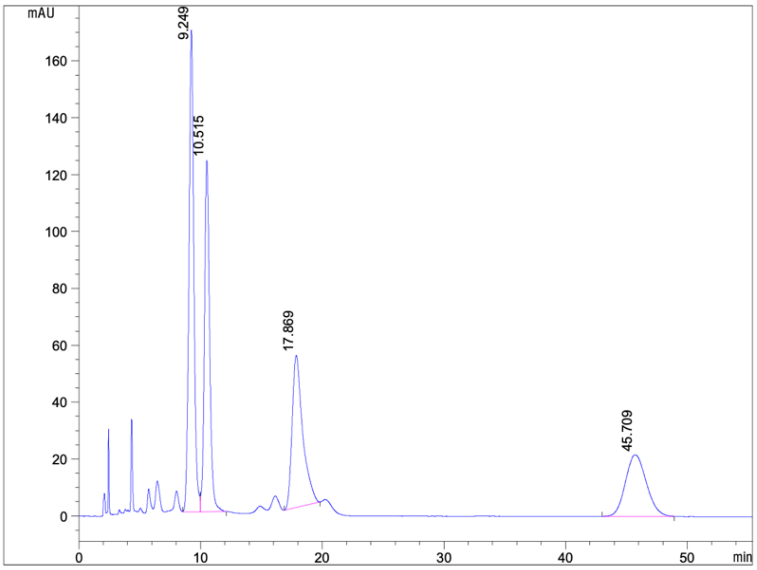

Signal 1: VWD1 A, Wavelength=225 nm

Peak #	RT [min]	Type	Width [min]	Area	Area %	Name
1	9.249	VV	0.420	4748.106	33.337	
2	10.515	VB	0.452	3663.496	25.722	
3	17.869	BB	0.896	3251.278	22.828	
4	45.709	MM	1.989	2579.725	18.113	

Extra 23. The HPLC chromatogram of **24** for Table 2, entry 8.

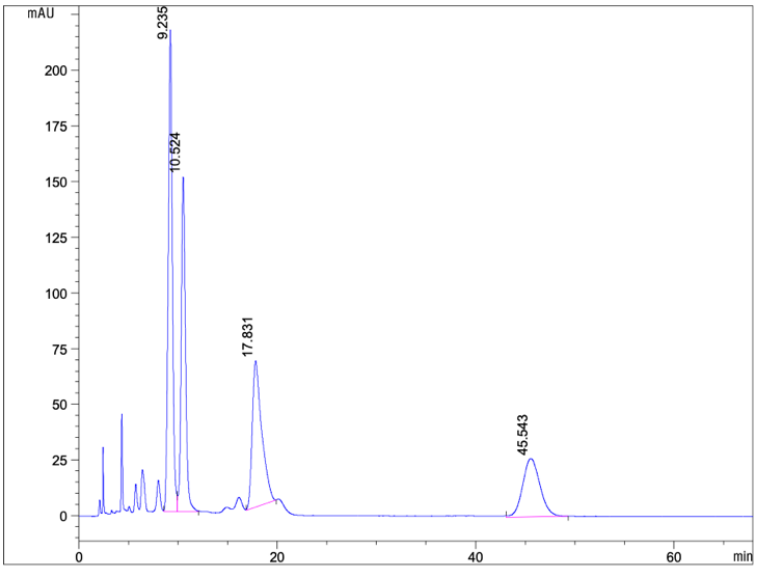

Signal 1: VWD1 A, Wavelength=225 nm

Peak #	RT [min]	Type	Width [min]	Area	Area %	Name
1	9.235	MF	0.485	6297.979	34.264	
2	10.524	FM	0.503	4539.736	24.698	
3	17.831	MM	1.105	4359.566	23.718	
4	45.543	MM	2.026	3183.562	17.320	

Extra 24. The HPLC chromatogram of **24** for Table 2, entry 9.

Annex
to Rector's directive No 1-8/17 of 7 April 2020

Non-exclusive licence for reproduction and publication of a graduation thesis[1]

I Rasmus Käsper

1. grant Tallinn University of Technology free licence (non-exclusive licence) for my thesis Development of Asymmetric Photochemical Reaction of Electron-Rich Cyclopropanols and Electron-Deficient Alkenes,

supervised by Anastasiya Krech,

1.1 to be reproduced for the purposes of preservation and electronic publication of the graduation thesis, incl. to be entered in the digital collection of the library of Tallinn University of Technology until expiry of the term of copyright;

1.2 to be published via the web of Tallinn University of Technology, incl. to be entered in the digital collection of the library of Tallinn University of Technology until expiry of the term of copyright.

2. I am aware that the author also retains the rights specified in clause 1 of the non-exclusive licence.

3. I confirm that granting the non-exclusive licence does not infringe other persons' intellectual property rights, the rights arising from the Personal Data Protection Act or rights arising from other legislation.

__27.05.2024__ (date)

[1] *The non-exclusive licence is not valid during the validity of access restriction indicated in the student's application for restriction on access to the graduation thesis that has been signed by the school's dean, except in case of the university's right to reproduce the thesis for preservation purposes only. If a graduation thesis is based on the joint creative activity of two or more persons and the co-author(s) has/have not granted, by the set deadline, the student defending his/her graduation thesis consent to reproduce and publish the graduation thesis in compliance with clauses 1.1 and 1.2 of the non-exclusive licence, the non-exclusive license shall not be valid for the period.*

Tallinn 2024